Mechanical behavior of bio-based concrete under various loadings and factors affecting its mechanical properties at the composite scale: A state-of-the-art review

Rafik Bardouh, Evelyne Toussaint, Sofiane Amziane, Sandrine Marceau

Cleaner Engineering and Technology 23 (2024) 100819

Contents lists available at ScienceDirect

Cleaner Engineering and Technology

journal homepage: www.sciencedirect.com/journal/cleaner-engineering-and-technology

Mechanical behavior of bio-based concrete under various loadings and factors affecting its mechanical properties at the composite scale: A state-of-the-art review

Rafik Bardouh [a], Evelyne Toussaint [a], Sofiane Amziane [a,*], Sandrine Marceau [b]

[a] Clermont Auvergne INP, Institut Pascal, UMR 6602 - UCA/CNRS, 63178, Aubière, France
[b] Université Gustave Eiffel, MAST-CPDM, 77454, Marne-la-Vallée, CEDEX 2, France

ARTICLE INFO

Keywords:
Plant-based concrete
Mechanical properties
Compression
Flexion
Shear
Physicochemical interactions
Plant aggregates
Mechanical behavior

ABSTRACT

The utilization of environmentally friendly materials derived from agricultural sources is becoming more prevalent in the construction industry. Many studies have already been conducted on various agro-resources, providing a variety of information on the characteristics of botanical aggregates and bio-based concrete. However, the prediction of the mechanical behavior of bio-based concrete remains complex owing to the various factors that influence its properties. Hence, it is crucial to collect a multitude of diverse information scattered throughout the literature regarding the mechanical response of bio-based materials under different loading conditions.

This paper review aims to evaluate the mechanical behavior law and mechanical properties of bio-based concrete under various loadings (compression, flexion, and shear) in accordance with multi-plant-aggregates and different mineral binders. The literature has provided around 120 papers listing a compilation of 18 plant aggregates sourced from various origins that are utilized in plant-based concrete. On the other side, a few types of aggregates and binders were introduced in the literature regarding the mechanical behavior of bio-based concrete. Several factors can affect the mechanical properties of bio-based concrete at the composite scale such as the formulation, the casting process (energy), the curing conditions, the morphology of the aggregates, the density, the porosity, the mineral matrix properties, and particles/binder physicochemical interactions. Hence, this paper elaborates on a conceptual understanding that focuses on the mechanical response of bio-based concrete in relation to the various influencing factors up to the application of these materials in building sector.

1. Introduction

Nowadays, buildings roughly contribute to 1/3 of the world's total energy consumption and global carbon emissions (Transition to Sustainable Buildings). The statement of the World Green Building Council was clear, to effectively align with the Paris Agreement's goals and achieve complete decarbonization by 2050 while ensuring global warming remains below 1.5°, the building and construction sector must address embodied emissions throughout the entire lifecycle of buildings ("WGBW19," 2019).

Biomass burning is a critical environmental issue since it pollutes the air as open-field burnings of biomass in India and China reached 84 and 10 Tg (Terra gram = 10^{12} g), respectively, causing severe health problems (Zhang et al., 2016, 2017). Accordingly, a sustainable method for the disposal of biomass residues derived from lignocellulosic plants, obtained from agricultural or forestry sources is warranted in the construction sector (Cuenca et al., 2013; Sellami et al., 2013). Many lignocellulosic aggregates have been investigated for the production of bio-based concrete, as listed in Table 1. These lignocellulosic aggregates were mixed either with organic binders such as starch (Benitha Sandrine et al., 2015) or mineral binders such as Portland cement, prompt natural cement (Collet et al., 2015), hydraulic lime (Hirst et al., 2010), non-hydraulic or calcic lime (de Bruijn, 2008), commercial lime (Tronet et al., 2016), hydraulic lime mixed with Tradical 70 (Boutin et al., 2006), pumice lime (Nozahic et al., 2012), clay (Mazhoud et al., 2017), gypsum, geopolymer (Ahmad et al., 2021), magnesium phosphate cement and alkali-activated cenosphere (Kristombu Baduge et al., 2019).

Integrating biomass aggregates into construction offers multiple

* Corresponding author.
E-mail address: sofiane.amziane@uca.fr (S. Amziane).

https://doi.org/10.1016/j.clet.2024.100819
Received 1 August 2024; Received in revised form 24 September 2024; Accepted 5 October 2024
Available online 13 October 2024

Abbreviations list

Apparatus modulus (Eini), 19
Apparent modulus (Ea1), 8
Axial strain rate (ε axi), 8
Barely straw (BS), 6
Binder-to-aggregate ratio (B/A), 25
Bulging and crushing failure mode (FM2), 11
Calcium-silica-hydrates C-S-H, 17
Change in deflection (ΔS), 22
Change in Load (ΔF), 22
Cohesion (C), 23
Corn cob (CC), 6
Elastic modulus (EC), 20 (Ecyc), 19 (Ee), 8
Flexural modulus (Eelast), 22
Fourier Transform Infrared Spectroscopy (FTIR), 17
Hardening modulus (Etan), 19
Hemp (H), 6
Hempcrete (HLC), 2
Interfacial transition zone (ITZ), 29
Lateral deformation (εlat), 8
Lavender straws (LS), 17
Length of the specimen (L), 22
Lime rice-husk concrete (LRC), 11
Lime-hemp concrete (LHC), 11
Longitudinal deformation (εlong), 8
Maximum compressive stress (σmax), 4
Maximum flexural load Fmax, 10
Maximum friction angle (ϕp), 23
Peak deviatoric stress (q), 23
Quarry fines derived from aggregates washing procedure (FWAS), 6
Ratio of deviatoric stress to mean effective pressure (M′), 23
Relative humidity (RH), 28
Secondary apparent modulus (Ea2), 8
shear band failure mode (FM1), 11
sunflower bark and pith with medium density (SBPD5), 7
Sunflower barks (SB), 17
sunflower pith concrete with low density (SPD2), 7
Thickness of the specimen (h), 22
Ultimate strength (σu), 5
Width of the specimen (b), 22
Young's modulus (E), 4

Table 1
Classification of various plant-aggregates used in the literature.

Family	Plants	Fraction	References
Wastes of plant's fiber	Hemp	Shiv	(Arnaud and Gourlay, 2012; Nguyen et al., 2009, 2010; Tronet et al., 2016; Véronique, 2005)
	Flax	Shiv	(Benmahiddine et al., 2020; Garikapati and Sadeghian, 2020)
	coconut	Coir	(Asasutjarit et al., 2007; Lertwattanaruk and Suntijitto, 2015)
Residues of wood transformation	Wood	chip	(Akkaoui et al., 2017; Al Rim et al., 1999; Bouguerra et al., 1998a)
Cereal stalks or straws	Barely	Straw	(Belhadj et al., 2016; Giroudon et al., 2019; Laborel-Préneron et al., 2017)
	Wheat	Straw	(Bouasker et al., 2014; Viel et al., 2018)
	Corn	Stalk	(Ahmad et al., 2018, 2021)
	Rice	Straw	Morsy (2011)
Oilseed plant straws	Sunflower	Stem	(Abbas et al., 2020; Magniont et al., 2012)
		stalk	Brouard et al. (2018)
	Rape	Straw	(Brouard et al., 2017, 2018)
Other cereal plants waste than straws	Corn	Cob	(Laborel-Préneron et al., 2017, 2018)
	Rice	Husk	Jauberthie et al. (2003)
Wild plants	Diss	Stem	(Merzoud, 2011; Sellami et al., 2013)
	Bamboo	Stem	(Corrêa et al., 2015; Park et al., 2019)
Sugar remnants	Sugar cane	Bagasse	("Agricultural Waste Materials as Thermal Insulation for TH," n.d.)
	Sugar beet	pulp	Costantine et al. (2020)
Bioenergy crop remnants	Miscanthus	Stem	(Acikel, 2011; Chen et al., 2017)
Scented plant straws	Lavender	Straw	Giroudon et al. (2019)

benefits, including carbon-negative properties, low density, sustainability, and improved indoor comfort through humidity control, thermal regulation, and acoustic insulation (Amziane and Collet, 2017; Bakkour et al., 2024; Bouguerra et al., 1998b; Hirst et al., 2010) For instance, 1 m^2 of hemp concrete with 25 mm thickness can store up to 35 kg of CO_2 over 100 years (Boutin et al., 2006). In addition, biomass aggregates enhance corrosion resistance when incorporated into ordinary concrete, particularly in the case of bio ashes like wheat straw and banana leaf, which help mitigate the corrosion rate (Thomas et al., 2021). However, the main problem that limits the durability of bio-based materials is the chemical degradation of lignocellulosic aggregates in an alkaline medium (Vo and Navard, 2016). In this regard, some treatments were found to enhance the durability of bio-based concrete including coating and impregnation of lignocellulosic aggregates by epoxy and adhesives, chemical or physical treatments, and even cementitious matrix modifications (Vo and Navard, 2016).

The primary issue with bio-based concrete is its inherent challenge related to low mechanical strength. Across different studies, HLC (hemp-lime concrete) exhibited a compressive strength of less than 2 MPa (Arnaud and Gourlay, 2012; de Bruijn et al., 2009; Elfordy et al., 2008; Jalali et al., 2006; kioy, 2005). Likewise, similar ranges of compressive strength were found for other types of bio-based concrete containing the following plant-by crops as aggregates: barely straw (Giroudon et al., 2019; Laborel-Préneron et al., 2017), rice husk (Chabannes et al., 2015), corn cob (Laborel-Préneron et al., 2017), sunflower bark (Lagouin et al., 2019), sunflower pith (Magniont et al., 2012), and maize (Lagouin et al., 2019). The low compressive strength along with a poor Young's modulus, indicates that this composite material is unsuitable for structural applications (Arnaud and Gourlay, 2012; kioy, 2005; Tronet et al., 2016; Véronique, 2005). This finding was explained by (Bouloc, 2006) to the high flexibility of aggregates, and their imperfect arrangement within the material. Besides the composition of binders, (Nguyen et al., 2009, 2010) observed a relatively high compressive stress of hemp concrete within the range of 2.65–3.57 MPa. This was attributed to the increased compaction pressure during casting, aimed at reducing voids within the material. In the same context, (Tronet et al., 2016) obtained a compressive stress of as high as 4.74 MPa for a casting stress of 6.7 MPa. Another study by (Tronet et al., 2011) revealed a compressive strength of 7 MPa at 7.5% of strain as the highest value of compressive strength of LHC reported in the literature. However, relatively superior compressive strength values were observed for bio-based specimens made with aggregates like miscanthus, corn stalk, and rice straw. For instance, miscanthus concrete reached up to 38 MPa in compressive strength making it suitable for structural applications under some formulations and physical treatments of the aggregates (Acikel, 2011). To this end, the

physical and mechanical properties of some treated aggregates can significantly alter the potential use of bio-based materials.

Bio-based concrete exhibited similarly low flexural resilience and strength within the range of 0.1–0.4 MPa (Elfordy et al., 2008; Jami et al., 2019; Murphy et al., 2010; Walker et al., 2014). However, the flexural strength of hempcrete under some formulations validates the Masonry Standards Joint Committee of a bare minimum flexural strength of 0.21 MPa ("TMS 402/602-08 Building Code Requirements and Specification for Masonry Structures, 2008," n.d.). The evolution of flexural modulus differs from that of Young's modulus as function of aggregate content. Flexural modulus tends to increase as aggregate content increases up to some extent (Agossou and Amziane, 2023; Al Rim et al., 1999).

In contrast to compressive and flexural loadings, only pair of studies in existing literature have assessed the shear properties of bio-based concrete (Chabannes et al., 2017; Youssef et al., 2015). Only two types of plant-based concrete were studied under shear loading: hemp and rice-husk concrete (Chabannes et al., 2017). The peak deviatoric stress for hemp-lime concrete and rice husk concrete was about 3.3 MPa and 1.75 MPa, respectively. It must be noted that the deviatoric stress depends to a large extent on the confining pressure during the shear test (Chabannes et al., 2017; Youssef et al., 2015). However, shear modulus depends to a large extent on the failure mode, since specimens that failed under shear banding exhibited higher shear modulus than specimens that failed under bulging (Chabannes et al., 2017).

Hereinafter, it is crucial to investigate the factors that may affect the mechanical parameters of bio-based concrete. Due to the extensive diversity of bio-aggregates, the characteristics of the same bio-aggregate might vary depending on its origin (Stevulova et al., 2013). The variability of bio-based concrete properties has 2 origins: intrinsic variability of the aggregates themselves (microstructure, porosity, density, water absorption), and uncertainty caused by insufficient information with respect to their mechanical performance (Niyigena et al., 2016). To mitigate the uncertainty of the biomass properties, specimens must undergo consistent drying conditions, follow a standardized protocol for aggregate sieving and casting process, ensure high-accuracy mechanical testing, and use a uniform method to identify the mechanical properties among the different specimens. Additionally, combining specimens results for scatter and goodness-of-fit analyses based on log-normal distribution is recommended (Niyigena et al., 2016).

This paper review aims to offer a conceptual insight into the mechanical response and properties of bio-based concrete, specifically focusing on functional aspects under various types of loading, including compression, flexion, and shear. This review also covers the numerous factors that influence the mechanical properties of bio-based concrete. These parameters can be dispatched into five categories. Firstly, the composition's nature, including the characteristics of the bio-aggregates, (sizing, density, water absorption, porosity) (Arnaud and Gourlay, 2012; Stevulova et al., 2012; Véronique, 2005), and the type of binders (de Bruijn et al., 2009; Hirst et al., 2010), secondly, the formulation process (Nguyen et al., 2009; Tronet et al., 2016), thirdly, physicochemical interactions between aggregates and mineral binders (Bourdot et al., 2019; Diquélou et al., 2015), fourthly, the casting methodology including the casting energy (Elfordy et al., 2008; Tronet et al., 2016) and the aggregates' orientation (Huang et al., 2022; Youssef et al., 2015), and lastly the curing conditions of bio-based materials (Arnaud and Gourlay, 2012). Regarding the diversity in the mechanical characteristics of bio-based concrete, several studies were performed including literature reviews addressing the influence of certain factors on the properties of these bio-ecological materials (Lagouin et al., 2019; Sáez-Pérez et al., 2020).

Hence, the literature selected for this review paper was carefully chosen from various range of references, with particular emphasis on the mechanical behavior of bio-based concrete. The present manuscript is divided into four main sections. The first section examines the mechanical response of bio-based concrete to different types of mechanical loading (compression, flexion, and shear). The second part elaborated on the mechanical performance of these materials according to the aforementioned various loading types. The third section lists a condensed overview of the various factors that can influence the mechanical properties of bio-based concrete at the composite scale. The last section elaborated on the application of bio-based concrete with a key connection to the mechanical performance of these materials as listed in this review paper. The outstanding results of this paper will allow the authors to have a prediction on the mechanical law regarding the mix of bio-aggregates with a mineral binder. This review is the outcome of a comprehensive literature survey conducted as part of the "BIOUP" project that aims to make significant advances in understanding the macroscopic properties of bio-based concretes, depending on the nature, or the type of aggregates and mineral binders.

2. Mechanical response and deformability of bio-based concrete

2.1. Compressive behavior

In the literature, the compressive behavior of plant-based concrete has been evaluated through both monotonic and cyclic compression tests, that were conducted on two different specimen shapes: cylindrical and cubic.

The compressive behavior of plant-based concrete is typically elastoplastic, showcasing a broad range of potential strains (Arnaud and Gourlay, 2012; Véronique, 2005). Accordingly, the stress-strain diagram of bio-based concrete consists of three distinct phases. The red hollow section in Fig. 1 marks the set-up phase at the test's start (Véronique, 2005).

During the initial phase, bio-based concrete demonstrates a linear quasi-elastic behavior (Arnaud and Gourlay, 2012; Elfordy et al., 2008; Walker et al., 2014), allowing for the determination of its Young's modulus (E). In this stage, the cement matrix, known for its greater rigidity compared to the bio-aggregates provides support for compressive stresses, resulting in slight strains being recorded. However, taking the small deformation theory to be true (strain up to 0.4 %), the modulus of elasticity E is determined as the gradient within the linear portion of the

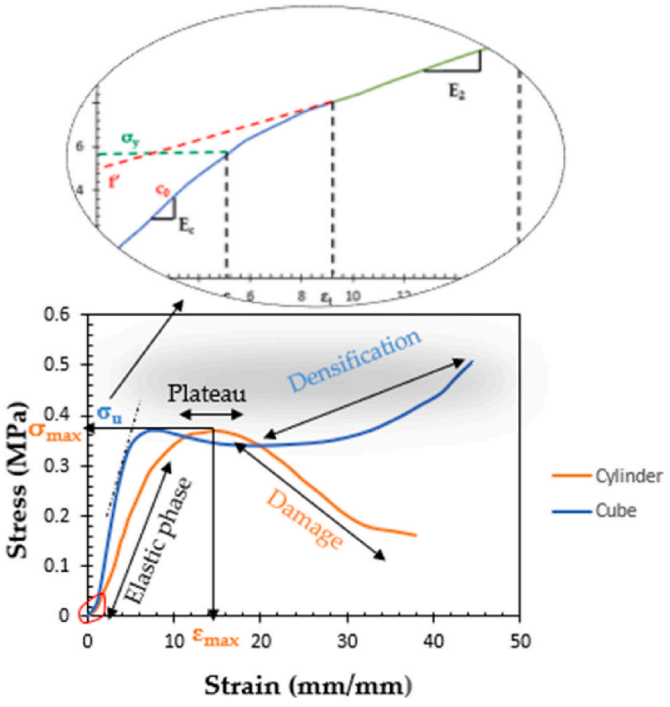

Fig. 1. Compressive behavior of plant-based concrete for different specimens' geometry (Pavia et al., 2015; Youssef et al., 2015).

stress-strain curve, as per Hooke's law (Véronique, 2005).

In the second phase, bio-based concrete exhibits an elastoplastic response. This phase is characterized by a progressive inflection, described by a slower increase in stress. This leads to the propagation of stress accentuation zones around the aggregates, resulting in gradual cracking of the binder matrix. As the material undergoes greater strain, particles crush gradually, culminating in the brittle failure of the binder (Arnaud and Gourlay, 2012; kioy, 2005; Véronique, 2005). This permanent plastic strain is evident in cyclic (loading-unloading) tests. Generally, the high porosity of plant aggregates allows for greater deformation, unlike traditional mineral-based concrete, where the aggregates are considered non-deformable. This phase, often referred to as the ''plateau" in literature, indicates a very slow increase in stress despite higher strain levels (Véronique, 2005; Walker et al., 2014). (Arnaud and Gourlay, 2012) demonstrated that the length of the post-peak plateau phase is directly related to the binder content in hemp concrete; lower binder content extends this phase due to the weaker setting of the mineral binder. The stress-strain curve eventually reaches its peak, representing the compressive stress (σ_{max} of the orange curve in Fig. 1), with the maximum strain occurring at this point, as shown in Fig. 1.

The third phase of the curve was not common among all plant-based concrete. For instance, several studies highlighted that the third phase in the mechanical behavior of bio-based concrete relies to a large extent on the geometry of the specimen (Glouannec et al., 2011; Pavia et al., 2015) (See Fig. 1). In this context, cylindrical specimens indicate complete damage to the binder matrix, rendering it non-functional in terms of mechanical support (orange curve in Fig. 1) (Arnaud and Gourlay, 2012). At this stage, the plant aggregates primarily bear the compressive stresses. As the particles are less rigid than the binder, strain levels increase while stress levels decrease. A distinct behavior of wood concrete in the third phase was remarked by (Akkaoui et al., 2017) as a plateau phase occurred after the peak stress. This plateau corresponds to the densification of the aggregate structure, resulting in increased density and closure of intergranular and possibly intragranular porosities. Conversely, several authors have observed a different mechanical response for cubic specimens characterized by a rapid stress increase with strain during the third phase, signifying densification or plastic hardening (see blue curve in Fig. 1) (Elfordy et al., 2008; Walker et al., 2014; Youssef et al., 2015). Indeed, (Akkaoui et al., 2017) attributed the densification response obtained in the third phase to the low binder content in the wood-concrete configurations. The particles are surrounded by a fine coating of cement paste, making the particle's fraction significant in supporting the load. (Elfordy et al., 2008) explained the observed densification by the squeezing of shives, which enhances the rigidity of bio-based concrete by increasing structural wall contact, thereby improving the mechanical properties. According to the authors (Elfordy et al., 2008; Walker et al., 2014), the σ_u ultimate strength of the compressive behavior corresponds to the debut of the plastic strain (σ_u of the blue curve in Fig. 1). Their methodology of calculation considered findings beyond the elastic strain limit, where deformation increases the stress without causing the specimen to fracture. This methodology was further elaborated by (Lecompte et al., 2015) based on the Yield strength as sketched in Fig. 1. This phenomenon is due to the irreversibility aspect of porous materials under compaction, similar to materials with high porosity when subjected to compression loading, restricted compression, or pressing indentation(Hirth and Tullis, 1989; Tancret and Osterstock, 2003).

Since the mechanical response of bio-based concrete is anisotropic (Nozahic et al., 2012; Véronique, 2005; Youssef et al., 2015), the fabrication process of cubic elements imparts to a large extent the tendency of the blue curve in Fig. 1. By default, layer-by-layer compaction induced an orthogonal orientation of the aggregates with respect to the compaction direction (Williams et al., 2016). However, stratification of the plant-based concrete occurred in other directions and encouraged the aggregates to orientate in a radial direction (Huang et al., 2022). Indeed, two different orientations of aggregates will result after the compaction: parallel to the casting or compaction direction, and orthogonal to the compacting direction as shown in Fig. 2. In this regard, it is worth mentioning that the mechanical tendency of the blue curve in Fig. 1 is only valid for cubic specimens with aggregates oriented perpendicularly to the compaction direction. The difference in mechanical tendency (mechanical strength 10 times higher for perpendicularly oriented specimens at relatively higher strain) between parallel-oriented specimens (blue curve in Fig. 2) and perpendicularly oriented specimens (orange curve in Fig. 2) was explained in previous studies (Huang et al., 2022; Nozahic et al., 2012; Youssef et al., 2015). According to (Youssef et al., 2015) the poor mechanical characteristics of parallel-oriented bio-based concrete stem from the early failure mechanism described by collapse and buckling between the layers of the specimen. This assumption was reported by one of the hypotheses of (Nozahic et al., 2012), where the authors elaborated the brittle behavior observed in parallel-oriented specimens to the encounter of plant particles with longitudinal direction under loading. This interaction led to the rapid crushing of particles due to interface shearing. In this context, perpendicular-oriented specimens evaluate the actual strength of the material whereas parallel-oriented specimens evaluate the strength of the coating interface between particles and cement paste. Indeed, the interface coating strength can be enhanced by chemical treatments (Nozahic and Amziane, 2012; Sedan et al., 2008). For instance, (Nozahic and Amziane, 2012) found that the maximum interfacial shear stress increased by 66% for $Ca(Oh)_2$ treated sunflowers compared to raw sunflowers.

The compressive behavior of bio-based concrete is notably affected by the nature of the bio-aggregated. Given this context, (Laborel-Préneron et al., 2017) evaluated the effect of several plant particles (S: barely straw; H: hemp; CC: corn cob) on the mechanical response and properties of earth-based materials using soil made of quarry fines derived from aggregates washing procedure (FWAS) as illustrated in Fig. 3.

The multiple curves illustrated in Fig. 3 correspond to the fluctuation in aggregate sizing (variable lengths used) and the numbers (3 % and 6 %) refer to the proportions of aggregates in each mixture. Generally, the ductility of earth-based composites markedly improved with the inclusion of bio-aggregates. Indeed, composites with Barely straw (S3 & S6) exhibited a very high strain rate at maximum stress compared to the other two composites thanks to its high compressibility. Yet, in structural application for buildings, such material distortions (19.9% of strain for S6) are intolerable (Laborel-Préneron et al., 2017). As a result, the strain was confined to 1.5%, and its related compressive stress was maintained to ensure a strain suitable for the desired application as

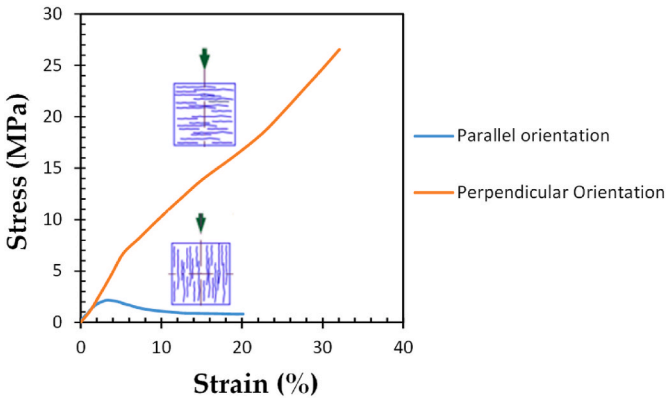

Fig. 2. Mechanical behavior of bio-based concrete according to the orientation of the particles with respect to compaction direction, (blue): Parallel orientation, (orange): Perpendicular orientation (Youssef et al., 2015). (For interpretation of the references to color in this figure legend, the reader is referred to the Web version of this article.)

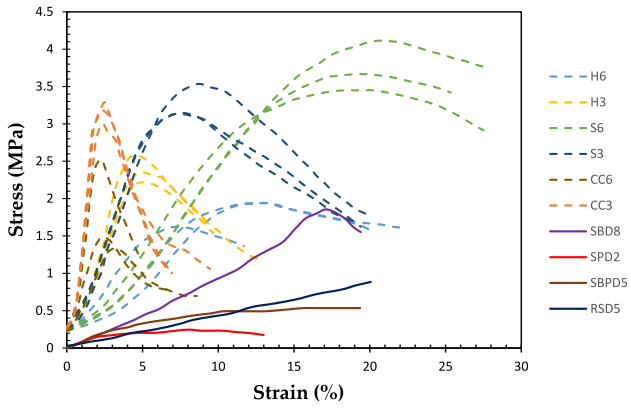

Fig. 3. Stress-strain curves for different plant-based composites (FWAS: quarry fine earth; S: barely straw; H: hemp; CC: corn cob, SBD8: sunflower bark at high density, RSD5: rape straw at medium density, SBPD: mix of sunflower bark and pith at medium density, SPD2: sunflower pith at low density) (Laborel-Préneron et al., 2017; Brouard et al., 2018).

described by (Véronique, 2005).

A direct correlation can be drawn between the increased content of aggregates and the decrease of the compressive stress. The values of the compressive stress decreased from 2.4 MPa to 3.2 MPa at 3% of aggregates proportion to 1.8 MPa for hemp (H) and corn cob (CC), respectively. This limitation in mechanical performance, associated with the inclusion of aggregates possessing poor mechanical properties, can be linked to the decline in bulk density observed when plant aggregate was added (Al Rim et al., 1999; Ghavami et al., 1999). However, an exception can be noticed regarding the compressive stress of barely straw composites (S) where this parameter increased from 3.3 MPa to 3.8 MPa between 3% and 6% of aggregate proportion, respectively. The authors (Laborel-Préneron et al., 2017) have attributed this evidence to two reasons: firstly the high compressibility of barely straw allowing a decrease in their porosity as strain increased, and secondly the more elongated shape of barely straw compared to hemp and corn cob (Laborel-Préneron et al., 2018). In a parallel research, (Brouard et al., 2018) evaluated the influence of various bio-based concrete having the same binder and mixing ratio but different densities. Indeed, D8 was the most dense configuration while D2 was the lowest. Similar elastoplastic behavior was remarked between sunflower pith concrete (SPD2) and the green concrete having a mixture of sunflower bark and pith (SBPD5) with the latter reaching a higher level of compressive strength due to the higher density of the mixture. However, rape straw concrete displayed a distinct compressive response, characterized by a steady rise in stress causing significant deformation without resulting in specimen failure.

Due to the slow hardening kinetics of plant-based concrete, influenced by the retarding effects of aggregate extracts on cement paste hydration (Diquélou et al., 2015), its mechanical behavior is closely linked to its age (Arnaud and Gourlay, 2012). Studies by (Arnaud and Gourlay, 2012; Véronique, 2005) examined the evolution of hemp concrete's mechanical properties over time to understand its hardening kinetics. Indeed, Fig. 4 illustrates that recently laid bio-based concrete (less than 6 months) is more deformable, making peak stress prediction difficult as it is mainly absorbed during the ductile phase (Véronique, 2005). Similar findings were reported by (Arnaud and Gourlay, 2012), where hemp concrete at an early age presents a very ductile behavior with a long post-peak plateau zone. This is attributed to the incomplete hydration and setting process of cement in plant-based concrete at an early age. (Arnaud and Gourlay, 2012; Véronique, 2005) explained this difference to the early-stage hydration of the cement, which had not yet reached its full setting inside a bio-based concrete. More particularly, the mechanical response at this early stage is mainly governed by the behavior of the particles rather than the binder.

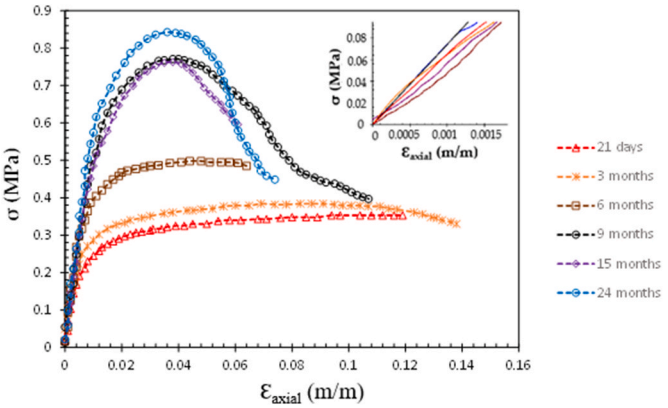

Fig. 4. Compressive behavior of hemp concrete according to the composite age (Véronique, 2005).

As bio-based concrete ages, the hydrates progressively interconnect, forming a continuous network that gradually transmits stresses (Arnaud and Gourlay, 2012). The properties of the mineral binder start to impart a greater influence on the mixture. This is evident in Fig. 4, where the compressive stress rises from 0.35 MPa at 21 days to 0.85 MPa at 24 months, while the corresponding strain (at maximum stress) decreases from 0.11 to 0.04 between 21 days and 24 months, respectively.

Hence, the variation in the mechanical behavior of plant-based concrete over time can be explained by the same consideration regarding the binder content. At low age, the mechanical response is primarily governed by the aggregates (lower compressive strength and higher ductility). Conversely, at high age, the mechanical properties more closely resemble those of the cement paste alone (high compressive strength and brittle behavior).

The cyclic compressive behavior of bio-based concrete (loading-unloading) can be divided into two zones based on the maximum stress ((1): prior-peak zone, and (2): beyond-peak zone) as shown in Fig. 5a. In the prior-peak zone (1), the material demonstrates orthotropic linear elastic response (Véronique, 2005), with residual deformation observed during loading-unloading cycles (Akkaoui et al., 2017). The residual deformation shows nearly linear changes in lateral strains relative to the longitudinal strain (Véronique, 2005). However, (Nguyen et al., 2010) further subdivided the prior-peak zone into 3 distinct phases (see Fig. 5b): (i) homogeneous elastic behavior, (ii) elastoplastic behavior with mineral binder and interface damage, and (iii) pronounced hardening with stress distribution to the aggregates and the initiation of their collapse (sealing the microstructure within the aggregates). It must be noted that the largest deformation was recorded during phase (iii). Thereafter, two mechanical parameters can be determined in phase (i) of the prior-peak zone: modulus of elasticity, defined as the gradient at the start of the curve $\sigma = f(\varepsilon)$, and the Poisson's coefficient which corresponds to the ratio lateral (ε_{lat}) to longitudinal deformation (ε_{long}) (Véronique, 2005). However, (Mazhoud et al., 2017) identified three different moduli during the loading-unloading cycles as shown in the crop section of Fig. 5a: the apparent modulus (Ea_1) at the initial part of the loading curve, the elastic modulus (E_e) during the linear part of discharging cycle, and a secondary apparent modulus (Ea_2) during the second loading cycle. After the end of loading-unloading cycles, the mechanical response exhibited an inflection tendency that progressively increases with strain (Véronique, 2005), reflecting non-linear deformation under compressive stress due to progressive binder matrix cracking (Nguyen et al., 2010). Once the peak stress is reached, the first zone ends, and the second, beyond-peak zone starts at a relatively high strain rate ($\varepsilon_{axi}5\%$). During the second zone, the binder matrix is completely damaged, and the aggregates primarily bear the load. Due to the significant variance in rigidity between bioparticles and cement paste

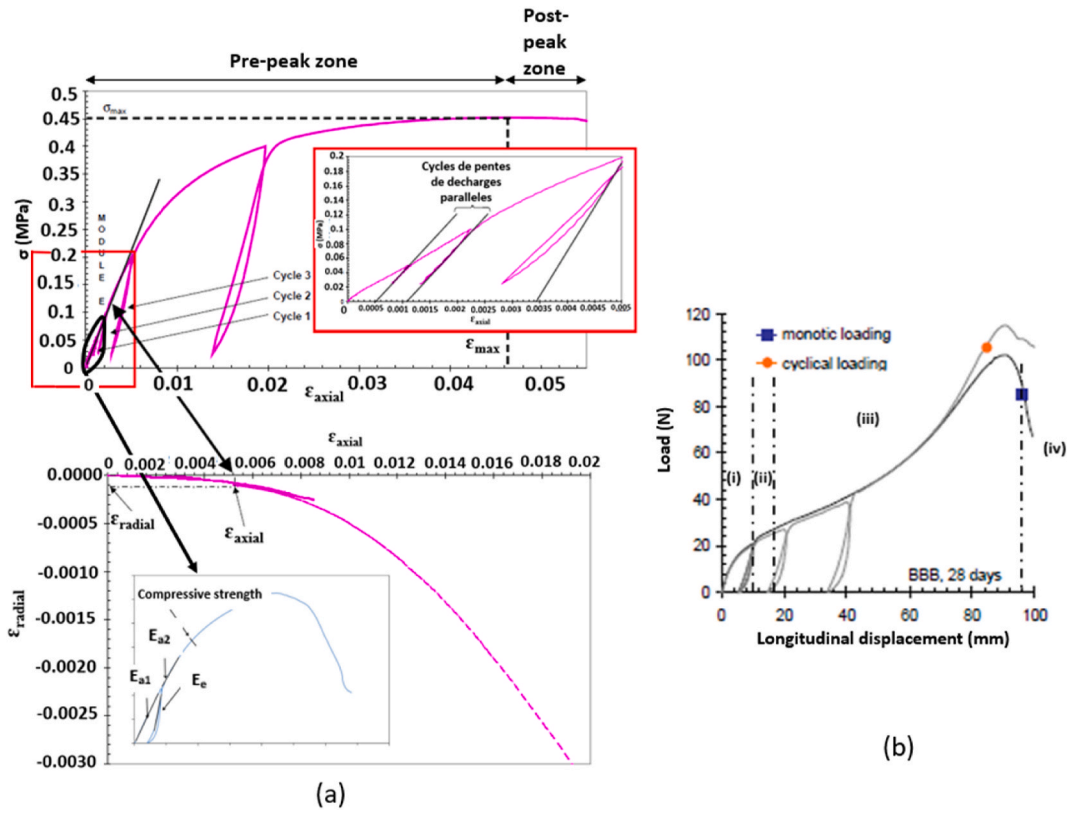

Fig. 5. (a): Cyclic compression curve for hemp concrete (Véronique, 2005), (b): Superposition of cyclic and monotonic loading curves of a compression test on hemp-lime concrete(Nguyen et al., 2010).

(ratio of 400), the stress supported by the aggregates is lower, resulting in a decreasing stress-strain curve in the post-peak zone.

2.2. Flexural behavior

The flexural response of bio-based concrete has been characterized through three-point and four-point bending tests. Various studies have discussed the flexural properties of plant-based and earth-based materials (Acikel, 2011; Belhadj et al., 2016; Chen et al., 2017; Elfordy et al., 2008; Garikapati and Sadeghian, 2020; Khazma et al., 2008; Laborel-Préneron et al., 2017; Mazhoud et al., 2017; Morsy, 2011; Murphy et al., 2010; Nguyen, 2010; Sassoni et al., 2014; Sassu et al., 2016; Walker et al., 2014).

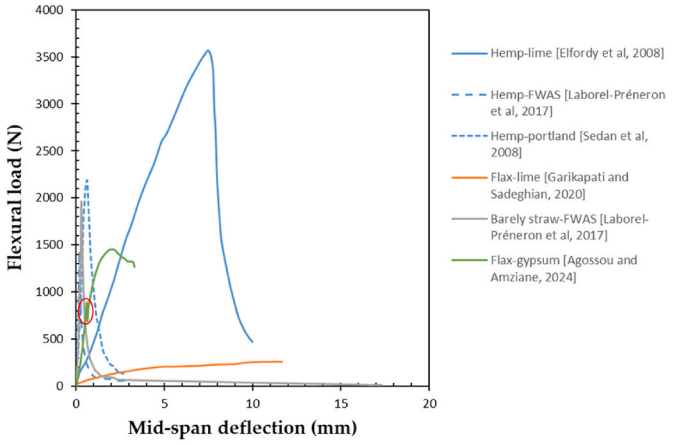

Fig. 6. Flexural behavior of bio-based concrete across different studies (Agossou and Amziane, 2023; Elfordy et al., 2008; Garikapati and Sadeghian, 2020; Laborel-Préneron et al., 2017; Sedan et al., 2008).

Fig. 6 illustrates the flexural response of several bio-based concrete under different loading conditions. These materials exhibit quasi-elastic behavior, described by two stages. In the initial stage, there is a nearly linear response, characterized by the matrix mainly carrying the load until a first macroscopic crack occurs, which emerges between the bottom of the specimen and the central axis of the prism (Le Troedec et al., 2007; Murphy et al., 2010; Sedan et al., 2008). This first crack aligns with the peak load reached, after which there's an abrupt decrease in flexural load due to the difference in rigidity between cement matrix and plant-aggregates, leading to specimen failure (Murphy et al., 2010; Walker et al., 2014). It must be noted that (Sedan et al., 2008) utilized hemp fiber in the composition of their mortars. In fact (Murphy et al., 2010), found that hemp concrete with low aggregate concentration (10 %) acts in a brittle manner after rupture, suggesting similar behavior between hemp fiber and shives at low proportions. In this regard, natural fiber-reinforced cement-based materials (green curve in Fig. 6) exhibit slight variations in flexural behavior compared to typical plant-based concrete. Several studies (Agossou and Amziane, 2023; Dalmay et al., 2010; Le Troedec et al., 2007) have identified three distinct phases of the flexural behavior of natural fiber mortars: a first linear elastic phase corresponding to the characteristics of the mineral matrix ending with the first crack as highlighted on the green curve in Fig. 6, a second phase of multiple cracks indicating stress transition from the cement matrix to the natural fibers where these latter's bridge microcracks on specimens inducing a controlled failure of the composite, and a third phase of progressive failure because of the failure at the interface fiber/matrix (Iucolano et al., 2015).

A similar tendency is observed in the flexural behavior of earth-based composites to that of bio-based materials. Indeed, (Laborel-Préneron et al., 2017) studied the effect of several bio-aggregates (S: barely straw; H: hemp) on the flexural behavior of earth bricks using quarry fines from aggregate washing processes (FWAS). The representative curves in Fig. 6

show increased ductility and deflection at failure due to residual strength storage. The authors (Laborel-Préneron et al., 2017) have explained the higher peak strain (strain computed at maximum deflection load) of earth composites with barely straw (S) compared to hemp (H) to the morphological characteristics of each aggregate. For instance, hemp particles were less elongated than barely straw particles (Laborel-Préneron et al., 2018). In a parallel study, (Murphy et al., 2010) observed that as aggregate content increases in the formulation of hemp concrete, better ductility is reached during failure. However, similar rigidity at the elastic phase exists between hemp and barely straw composites made with Portland cement and FWAS earth. Hemp-lime concrete showed lower rigidity in the elastic phase compared to other types of hemp concrete (Elfordy et al., 2008). The variabilities in flexural response between studies are due to differences in plant-based concrete formulation, specimen shape, and casting process. This later was unique in the research conducted by (Elfordy et al., 2008), where they used a projection process during casting, resulting in a substantial increase in the flexural stress of hemp-lime concrete as can be seen by the maximum load of the corresponding curve (F_{max}=3568 N) in Fig. 6. It can be noticed that flax-lime concrete (orange curve in Fig. 6) exhibited a different flexural behavior due to the addition of jute fabric mesh, causing stress concentration in the local area near the flax shives, thereby lowering flexural strength and rigidity (Garikapati and Sadeghian, 2020).

2.3. Shear behavior

It is essential to gain insight into the shear behavior of bio-based concrete, as shear failure is the most prevalent type of wall failure (Chabannes et al., 2017; Jami et al., 2019). Triaxial compression tests have been used to investigate this behavior, although studies are limited, primarily focusing was on hemp concrete and rice husk concrete (Chabannes et al., 2017; Youssef et al., 2015). A key factor in triaxial compression tests is the confining or lateral pressure, which consists of the vertical pressure applied by the piston as shown in Fig. 7a. The final assembly of the triaxial shear test is presented in Fig. 7b. The shear response of (a): lime-hemp concrete and (b): rice husk concrete is presented in Fig. 8 (Chabannes et al., 2017). Likewise, (Youssef et al., 2015) assessed the shear behavior of cubic cut hemp lime with different formulations M1 (W/B = 0.55, B/A = 1.8, and compactness = 0.37 MPa), M4 (W/B = 0.55 and B/A = 0.54, and compactness = 0.54 MPa)), and a confidential chanvribloc as shown in Fig. 9 (a), (b), and (c), respectively. It must be noted that the lower and upper terms in Fig. 9 correspond to the location of the cut portion of a hardened hemp lime cylinder whether at the top or at the bottom of the cylinder. The discrepancy in shear behavior for hemp-lime concrete between the two studies was due to several factors such as specimen shape, strain computation, confining pressure, and mixing design. For instance, (Youssef et al., 2015) tested cubic specimens, whereas (Chabannes et al., 2017) tested cylindrical specimens. In addition, the strain computed by (Chabannes et al., 2017) was an axial strain whereas (Youssef et al., 2015) computed an angular strain. However, common trends in the shear behavior of chanvribloc and LHC (lime -hemp concrete) include an initial elastic phase up to a small range of strain (lower than 2%), followed by a plastic phase (strain hardening). (Chabannes et al., 2017) observed an additional two phases for LHC and LRC: a plateau phase (small increase in deviatoric stress under high axial strain rate increase), followed by a post-peak phase characterized by rapid softening. Nevertheless, both studies indicated that plant-based concrete performed in ductile response, suggesting its potential for structural application, particularly in dissipating energy during seismic events (Youssef et al., 2015).

Increasing confining pressure was found to enhance peak deviatoric, shear strength, and ductility in both studies as seen in Fig. 8(a) and (b) and Fig. 9 (c). For instance, a gain in deviatoric stress by 22% and 16 % was reached between 25 kPa and 150 kPa for LHC and LRC, respectively. The differences in shear behavior between LHC and LRC were attributed to their anisotropy, with LHC exhibiting a stratified arrangement leading to bulging failure, while LRC was more isotropic (Chabannes et al., 2017). LRC specimens presented a less ductile behavior than LHC specimens due to the intrinsic characteristics of rice husk, the distribution of particle sizing, and the ratio of voids between the aggregates. However, for high confining pressures (100 and 150 kPa), some LHC specimens exhibited brittle behavior marked by lower strain rates and higher elastic modulus, due to localized shear band failure mode (FM1). Those specimens were highlighted by a hollow circle for each representative curve as shown in Fig. 8 (a). This type of failure (shear band) was well known in the literature to cause a fast decline and softening response following the peak stress (Marri, 2010). Nonetheless, most of LHC specimens experienced bulging and crushing failure mode at their bottom part (mainly denoted FM2 in the authors' study (Chabannes et al., 2017)), attributed to density gradients and non-uniform distribution of pores along the specimen. This non-uniform distribution prompts the initiation of microcracks in the weaker lower half, resulting in densification in that region. In contrast, LRC specimens mostly experienced shear banding (FM1) except for one specimen that failed due to bulging (FM2), which showed significant strain hardening at a strain range from 3% to 18%, mitigating the plateau phase until failure.

3. Mechanical performance of bio-based concrete (strength and rigidity)

3.1. Properties under compressive loading

The mechanical properties of bio-based concrete under compressive

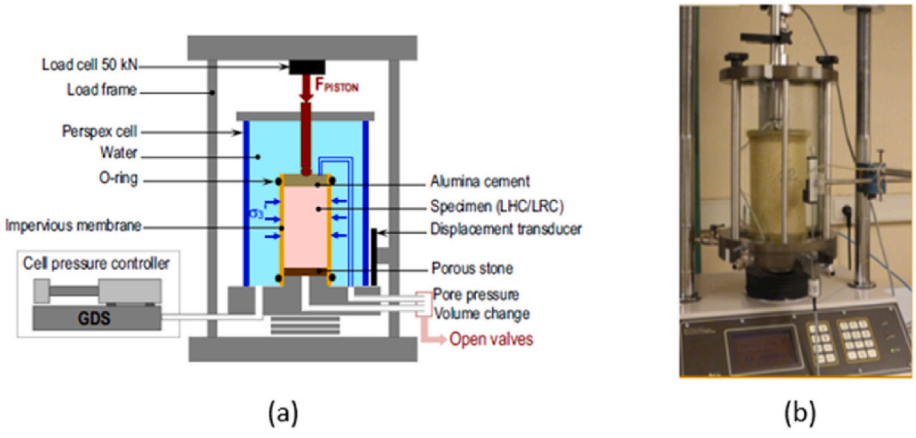

Fig. 7. (a): Schematic representation of triaxial shear test, (b): Final triaxial compression test set-up of the bio-based specimen (Chabannes et al., 2017).

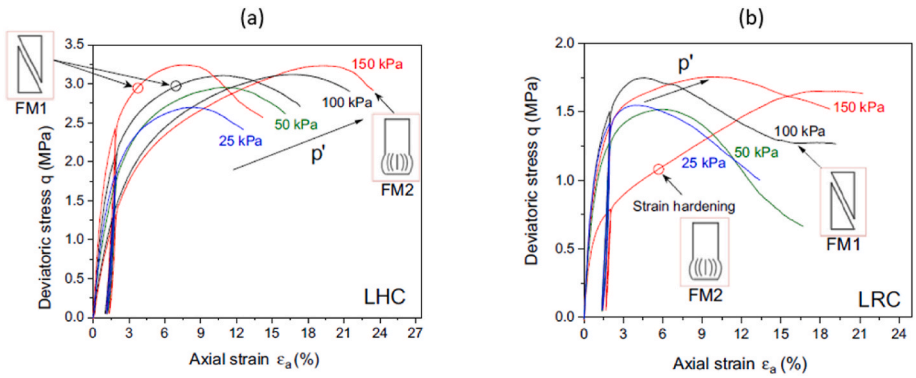

Fig. 8. Shear behavior of bio-based concrete under different confining pressures (a): hemp-lime concrete (LHC), (b): Rice husk concrete (LRC) (Chabannes et al., 2017).

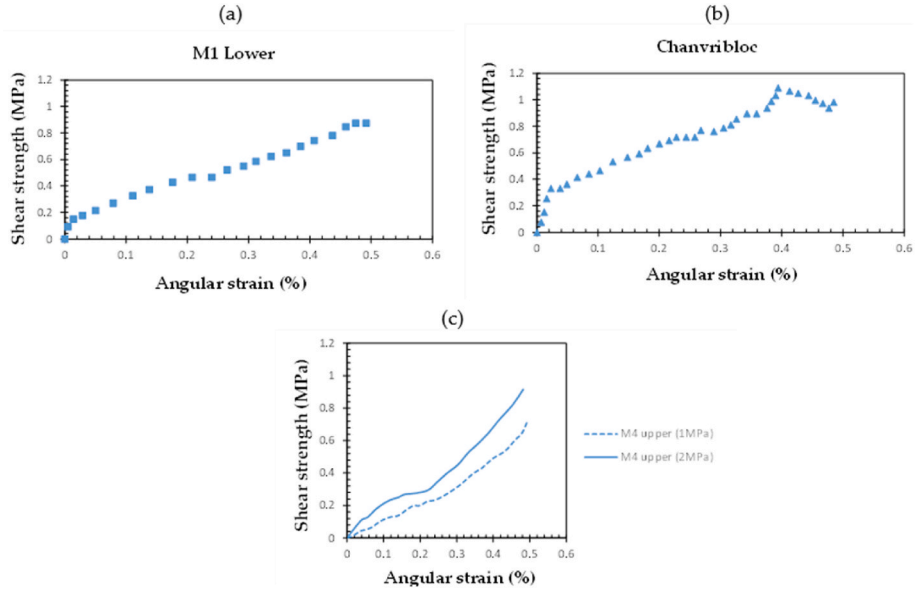

Fig. 9. Shear behavior of hemp concrete under various confining pressure for different formulations, (a): M1 lower (1 MPa), (b): Chanvribloc (0.2 MPa), (c): M4 upper (1 and 2 MPa) (Youssef et al., 2015).

loading examined in the literature are reported in Table 2. The variations of the mechanical parameters computed in the same study are due to several reasons such as the mix formulation of bio-based concrete, the methodology of assessing the properties, casting process, compaction energy, age of bio-based concrete, curing conditions, size of the particles, treatments on aggregates, and the type of mineral binder.

3.1.1. *Compressive strength*

The compressive strength emerges as a critical mechanical parameter in construction, denoting the material's ability to resist compressive loads without deformation or failure (Jami et al., 2019). Currently, there is no standardized procedure for measuring or identifying the compressive strength in compacting behavior (Mazhoud et al., 2017; Niyigena, 2016; Walker et al., 2014). Different methodologies have been used to determine this property. For instance, drawing from the model of (Lam and Teng, 2009), some studies (Elfordy et al., 2008; Lecompte et al., 2015; Mazhoud et al., 2017; Tronet et al., 2016; Walker et al., 2014) identify the compressive stress as the yield strength (at the depart of the elastic phase of the stress-strain curve). However, some studies proposed arbitrary characterization values of strain during elastic and plastic zones (1.5% and 7.5%) at which compressive stresses were computed (Nguyen, 2010; Nguyen et al., 2009, 2010; Tronet et al., 2011, 2016) with (Véronique, 2005) further explaining the choice of 1.5% to match the intended application of hemp concrete under compressive loads. In contrast, most studies on plant-based concrete report compressive strength as the ultimate strength (σ_{max}) reached by the material before failure (Arnaud and Gourlay, 2012; Chabannes et al., 2015; de Bruijn et al., 2009; Hirst et al., 2010; kioy, 2005; Véronique, 2005), providing easily discernible values of compressive stress due to the typical elastoplastic behavior as shown in Fig. 1 (orange curve). The compressive stress varies according to the mixture's formulation, casting process including the compacting energy, the type of constituents (mineral binders and aggregates), the shape of the specimen (cylindrical or cubic), and the material's age under storing conditions. Fig. 10 summarizes the compressive strength values for various bio-based concrete with respect to aggregate content. These multiple factors contribute to the complexity of comparing results between distinct studies.

A general trend can be observed with the decline in compressive stress as the bio-aggregates percentage increases. This pattern is linked to high pores and voids between and within formulations, leading to lighter green density (Niyigena et al., 2016; Véronique, 2005). Consequently, there is a direct correlation between low-density and low compressive stress. (Niyigena et al., 2018), further noted that elevated aggregate content enlarges the specific area of the aggregates, thereby leading to a weaker particle/binder interface and subsequently lowering

Table 2
Mechanical properties of bio-based concrete under compression.

Aggregates	Binder nature	Dry density (kg/m^3)	Compressive strength σ_c (MPa)	$\sigma_{1.5\%}$ (MPa)	$\sigma_{7.5\%}$ (MPa)	Young's modulus E (MPa)	References
Hemp hurds	Tradical PF 70[a]	684	0.3			10	Nguyen et al. (2009)
		963	–			40	
		850	–	1.58	3.57	131	Nguyen et al. (2010)
		670	–	1.34	2.65	113	
Hemp shives	NHL 3.5[b]	460	0.18	0.08	0.13	9	Arnaud and Gourlay (2012)
	NHL 3.5-Z[c]	480	0.31	0.21	0.27	36	
	NHL 3.5-Z[c]	480	0.31	0.21	0.27	36	
	NHL 2[d]	480	0.10–0.22	0.19	0.21	5–24	
	Tradical PF 70[a]	460–500	0.30–0.34	0.22	0.3	–	
	–	610	1.88	0.70	1.65	43	kioy (2005)
	–	830	1.98	0.86	1.82	52	
	T70[e]	356	0.3	0.21	0.35	14	Véronique (2005)
		391	0.35	0.22	0.39	44	
		504	0.7	0.57	–	15	
	Lime-based binder	–	–	1.5	3.2	120	Tronet et al. (2011)
				1.4	3.3	103	
				1.1	3.9	90	
				1	7	105	
	Tradical PF 70[a]	–	1.36	–	2	43	Tronet et al. (2016)
		–	1.63	–	3	51	
		–	2.13	0.2	4	70	
		–	4.74	2.2	7	147	
		–	3.95	1	9	122	
	Commercial lime-based binder	270–330	0.10–0.20	–	–	–	(Sutton et al., 2011)
	Patented MgO based binder with water-soluble vegetable protein	330	1.15	–	–	–	Sassoni et al. (2014)
	60% Dolomitic Lime +40%	540	0.266	–	–	–	Sinka et al. (2014)
	Metakaolin	397	0.154	–	–	–	
		330	0.133	–	–	–	
	Pure Dolomitic Lime	461	0.181	–	–	–	
		367	0.136	–	–	–	
		345	0.125	–	–	–	
	NHL3.5	643	0.414	–	–	12.495	Sassu et al. (2016)
		698	0.146	–	–	3.387	
	85% NHL+15% Portland cement	753	0.357	–	–	12.190	
	Portland cement	638	0.622	–	–	15.07	
	BCB Tradical[f]	351	0.675	–	–	16	Elfordy et al. (2008)
		387	0.675	–	–	26	
		417	0.45	–	–	24	
		461	0.78	–	–	34	
		481	0.8	–	–	35	
	Binders mix	360	0.2	–	–	–	Walker et al. (2014)
	Commercial mix	360	0.21	–	–	–	
	GGBS	360	0.13	–	–	–	
	GGBS + WR	360	0.14	–	–	–	
	Metakaolin	360	0.1	–	–	–	
	Metakaolin + WR	360	0.2				
	Hydrated + Hydraulic Lime	587–733	0.2	–	–	13.41	de Bruijn et al. (2009)
		587–733	0.15	–	–	12.65	
		587–733	0.44	–	–	17.4	
		587–733	0.83	–	–	28.01	
	Portland	587–733	0.55	–	–	49.4	
	THB[g]	221	0.025	–	–	3.3	(Hirst et al., 2010)
		278	0.05	–	–	3.7	
		342	0.18	–	–	12	
	Clay	509.48	0.48	–	–	26.12	Mazhoud et al. (2017)
		477.36	0.47	–	–	23.52	
		451.51	0.43	–	–	20.19	
		373.71	0.39	–	–	16.25	
	Stabilized Clay	577.41	0.68	–	–	55.97	
		524.60	0.64	–	–	48.28	
		475.22	0.58	–	–	36.56	
		410.28	0.47	–	–	25.96	
Hemp shives	Prompt natural cement	488.88	0.46	–	–	43.45	Niyigena et al. (2016)
		451.61	0.44	–	–	31.86	
		469.78	0.43	–	–	32.77	
		422.10	0.32	–	–	30.97	
	50% NHL5 + 50% flash calcined metakaolin	924.8	2.2	–	–	–	Magniont et al. (2012)
		630.3	0.3	–	–	–	
		533.6	0.2	–	–	–	
	Pumice lime	1184	2.14	–	–	–	Nozahic et al. (2012)

(*continued on next page*)

Table 2 (*continued*)

Aggregates	Binder nature	Dry density (kg/m^3)	Compressive strength σ_c (MPa)	$\sigma_{1.5\%}$ (MPa)	$\sigma_{7.5\%}$ (MPa)	Young's modulus E (MPa)	References
		1266	5.44	–	–	–	
	Green binder (wheat straw)	179.84	0.26	–	–	–	Viel et al. (2019)
		187.85	0.34	–	–	–	
		165.92	0.27	–	–	–	
		181.57	0.29	–	–	–	
cork	NHL 3.5	561	0.73	–	–	18.57	Sassu et al. (2016)
Rice husk	50% NHL3.5 + 50% cl90-S	625	0.33	–	–	45	Chabannes et al. (2015)
		666	0.31	–	–	51	
Flax shives	Tradical PF 70	638	1.19	–	–	–	Benmahiddine et al. (2020)
		541.2	0.8	–	–	–	
		468	0.53	–	–	–	
		664.6	0.91	–	–	–	
		549	0.74	–	–	–	
		460.9	0.61	–	–	–	
		643.8	0.91	–	–	–	
		550.8	0.79	–	–	–	
		469.4	0.59	–	–	–	
	CEM I 52.5	850	0.4	–	–	–	Khazma et al. (2008)
Wood chips	CPA-CEMII 32.5	–	0.19	–	–	249	Akkaoui et al. (2017)
		–	2	3	–	756	
		–	4.1	3.8	–	1900	
	CPA-CEMI 52.5	1170	–	–	–	–	Al Rim et al. (1999)
		1010	2.42–2.67	–	–	958	
		870	1.9–2.35	–	–	819	
		700	1.11–1.35	–	–	371	
		490	0.31–0.34	–	–	94	
	CPA-CEMI 52.5	1065	7	–	–	–	Bouguerra et al. (1998a)
		908	5	–	–	–	
		800	4	–	–	–	
		621	2.8	–	–	–	
Sunflower	50% NHL5 + 50% flash calcined metakaolin	1041.6	5.5	–	–		Magniont et al. (2012)
		777.2	3.5	–	–		
		670.4	2.2	–	–		
		576.4	1.1	–	–		
	Pumice-lime	1084	1.63	–	–	–	Nozahic et al. (2012)
		1204	4.68	–	–	–	
	Clay binder	235	0.19	0.08	0.12	3.5	Brouard et al. (2018)
		512	0.4	0.08	0.22	6.1	
		714	2.1	0.17	0.63	5.8	
	Lime-based binder	539.64	0.20	0.045	0.18	–	Lagouin et al. (2019)
	Metakaolin	511.07	0.32	0.132	0.32	–	
Barely straw	Sand cement	–	18	–	–	–	Belhadj et al. (2016)
		–	13	–	–	–	
		–	12	–	–	–	
	FWAS[h]	1519	3.3	0.7	–	62	(Giroudon et al., 2019;
		1195–1315	3.8	0.4	–	31	Laborel-Préneron et al., 2017)
		1520	2.1	0.6	–	43	Laborel-Préneron et al. (2017)
		1075	3.6	0.3	–	25	
Corn cob	FWAS[h]	1878	3.2	2.1	–	217	
		1754	1.8	1.3	–	102	
		1876	1.3	1.3	–	136	
		1654	1	0.9	–	69	
Miscanthus	Portland	1504	14.8	–	–	–	Chen et al. (2017)
		1406	11.0	–	–	–	
		1160	5.21	–	–	–	
		1520	23.14	–	–	–	
		1436	15.97	–	–	–	
		1340	10.78	–	–	–	
	CEMII 32.5	1840	37	–	–	–	(Acikel, 2011)
		1900	37	–	–	–	
		1840	46	–	–	–	
Lavender Straw	FWAS[h]	1772	3.7	1.8	–	134	Giroudon et al. (2019)
		1585	3.9	0.6	–	64	
Bamboo	Portland	–	13.55	–	–	13500	Park et al. (2019)
		–	5.76	–	–	5000	
		–	3.13	–	–	3200	
		–	15.01	–	–	16300	
		–	14.15	–	–	9800	
		–	8.99	–	–	5100	

(*continued on next page*)

Table 2 (*continued*)

Aggregates	Binder nature	Dry density (kg/m^3)	Compressive strength σ_c (MPa)	$\sigma_{1.5\%}$ (MPa)	$\sigma_{7.5\%}$ (MPa)	Young's modulus E (MPa)	References
		–	23.73	–	–	18900	
		–	19.04	–	–	12200	
		–	17.75	–	–	10300	
Rape straw	Clay binder	438	–	0.1	0.3	3.2	Brouard et al. (2018)
	Prompt natural cement	580	0.8	–	–	20	Sheridan et al. (2017)
		640	1.48	–	–	50	
Rice Straw	CEM I 52.5R	1200	9	–	–	–	Morsy (2011)
		1550	15	–	–	–	
		1600	18	–	–	–	
		1850	30	–	–	–	
Rice husk	CPA-CEM I 52.5	1110	20.6	–	–	1000	Jauberthie et al. (2003)
		1145	23.8	–	–	2600	
Maize	Lime-based binder	160	0.24	–	–	7.5	Abbas et al. (2020)
	Metakaolin	534.08	–	0.027	0.17	–	Lagouin et al. (2019)
Corn stalk	MgO-based binder	817	6.3	–	–	–	Ahmad et al. (2018)
		1048	9.4	–	–	–	
		1657	20.8	–	–	–	
		1854	28.4	–	–	–	

[a] 75% hydrated lime $Ca(OH)_2$, 15% hydraulic lime, 10% pozzolana.
[b] Natural hydraulic lime with a minimum compressive strength of 3.5 MPa.
[c] Natural hydraulic lime containing pozzolanic additives possessing a minimum compressive strength of 3.5 MPa.
[d] Natural hydraulic lime with a minimum compressive strength of 2 MPa.
[e] 63% air lime, 37% hydrated lime.
[f] 70% hydrated lime, 15% pozzolans, 15% hydraulic lime.
[g] 90% air lime with additional hydraulic components and other additives.
[h] Quarry fines earth from aggregate washing processes.

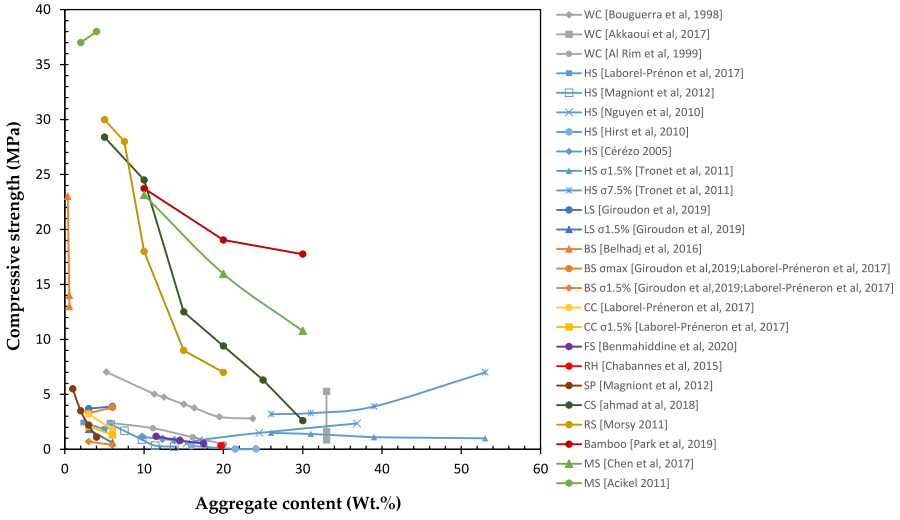

Fig. 10. Compressive stress of bio-based concrete and earth-based materials as a function of aggregate content across different studies (HS: hemp shives; WC: wood chips; LS: lavender straw; BS: barely straw; CC: corn cob; RH: rice husk; CS: corn stalk; MS: miscanthus stem; FS: flax shives; SP: sunflower pith; SB: sunflower bark; RS: rice straw, Maize; Bamboo.

the compressive stress.

Nevertheless, the impact of aggregate content on compressive stress varies across studies. Some researches (Acikel, 2011; Belhadj et al., 2016; Giroudon et al., 2019; Nguyen et al., 2010; Tronet et al., 2011) have noticed a rise in the compressive strength with higher aggregate. For instance, (Nguyen et al., 2010) noted that compressive strength increased with more aggregate content due to higher compaction pressure applied and the addition of more mineral binder to maintain a constant binder/aggregate ratio. Similarly, (Tronet et al., 2011) found that higher aggregate content led to increased compressive strength at high strain rate (7.5%) due to increased compaction stress needed to achieve the desired density for all specimens (816 kg/m^3). However, this increase in compressive strength is not limitless. In this regard, (Bouhicha et al., 2005) observed a rise in the compressive stress of soil composites up to 1.5% of barely straw, meanwhile, further increase resulted in a decline of compressive stress. Thus, optimizing the proportion of plant aggregates is crucial for enhancing mechanical properties.

Fig. 10 illustrates the compressive strength as a function of aggregate content for different bio-based specimens assessed in the literature. Bamboo concrete was the least influenced type by the increased aggregate content, due to a wet coating technique that improved compressive

strength compared to dry natural aggregates (Park et al., 2019). Hemp-lime concrete (LHC or hempcrete), stood out as the most examined type of bio-based concrete, with compressive strengths typically ranging from 0.2 MPa to 2 MPa (Arnaud and Gourlay, 2012; kioy, 2005; Magniont, 2010; Sinka et al., 2015; Sutton et al., 2011; Tronet et al., 2011; Véronique, 2005; Walker and Pavia, 2014). Indeed, this lightweight material has significantly lower compressive strength than traditional concrete blocks, about 1/20th (Sutton et al., 2011). Therefore, French professionals recommend tamped lime-hemp concrete walls and roofs to have a compressive strength of 0.3 MPa (Construire en chanvre. Règles professionnelles d'éxécution - SEBTP, n.d.; Tronet et al., 2016). Bouloc attributes LHC's low compressive strength to the non-perfect alignment of the shives, high aggregate pliability under deformation, and porous nature, applicable to other plant-based concretes using wood chips, flax shives, rice husk, sunflower stem, and corn cob (Bouloc, 2006). However, Wood concrete exhibited relatively higher compressive strength values (Akkaoui et al., 2017; Al Rim et al., 1999; Bouguerra et al., 1998a) than hemp concrete due to the higher density and physical properties of the wood chips compared to hemp shives. To this end, higher compressive strengths have been reported for LHC when higher compaction stresses are applied, indicating a higher density (Nguyen, 2010; Nguyen et al., 2009, 2010; Tronet et al., 2011, 2016). (Elfordy et al., 2008) also found a correlation between density (weight), compressive stress, and compactness. (Tronet et al., 2011) reported ultimate compressive strength up to 7 MPa and 9 MPa (Tronet et al., 2016) for hemp-lime concrete at higher strain rates (7.5%), due to its continuous ascending mechanical response which makes the identification of a stress peak complicated (Walker et al., 2014), unlike conventional elastoplastic behavior (Arnaud and Gourlay, 2012). In parallel studies on plant-based composites (Bourdot et al., 2019; Giroudon et al., 2019; Laborel-Préneron et al., 2017; Lagouin et al., 2019; Niyigena et al., 2018), other indicators of stresses in the elastic zone (strain of 1.5% and 5%) have been proposed to determine the compressive strength.

Other plant-based concretes like those using barely straw (Belhadj et al., 2016), miscanthus (Acikel, 2011; Chen et al., 2017), rice straw (Morsy, 2011), corn stalk (Ahmad et al., 2018), and bamboo (Park et al., 2019) demonstrated significantly higher compressive strength for the same aggregate content compared to hemp-lime concrete. This finding highlights that some of these bio-based concrete can be considered as load-bearing materials at a specific aggregate content below 7% followed by a refining and chemical treatment of the aggregates as in the case of miscanthus concrete that reached a 38 MPa at 5% of treated miscanthus particles (Acikel, 2011). In the same regard, corn stalk concrete exhibited compressive strength of around 25 MPa at 10% aggregate content, much higher than hemp-lime concrete's 2.1 MPa. (Ahmad et al., 2018) attributed this improvement to the high early strength of MgO-based binders and the strong interaction between undeformed corn stalk aggregates and the cement paste. The morphological parameters of the aggregates greatly impart the mechanical properties. For instance, some studies (Giroudon et al., 2019; Laborel-Préneron et al., 2017) found that the compressive strength of bio-based concrete for relatively longer aggregates increased by 0.5 MPa for barely straw and by 0.2 MPa for lavender straw, as the aggregate content increased from 3% to 6%, respectively. This evidence was related to the consolidation process of longer aggregates, owing to their high compressibility, thereby reducing porosity as strain increases (Laborel-Préneron et al., 2017, 2018). In addition, (Morsy, 2011) reported a compressive stress of 30 MPa for rice straw concrete at 5% of aggregate content, improved by NaOH treatments that removed non-cellulosic impurities. This, in turn, led to stronger chemical bonding and mechanical interlocking between straws and cementitious matrix.

Nevertheless, the rise in compressive stress did not reliably indicate the suitability of plant-based composites, as it also increased the corresponding strain (Ratsimbazafy et al., 2021). For instance, (Chabannes et al., 2017) noted greater unconfined compressive stress in hemp concrete compared to rice-husk concrete, accompanied by increased strain at maximum stress; 6% for hemp concrete versus 3% for rice husk concrete. This was attributed to the more compact granular skeleton of hemp shives and the higher inter-particle porosity in rice husk concrete (Chabannes et al., 2017).

Fig. 11 displays the compressive stress of bio-based concrete relative to the median aggregate length. No direct trend was remarked due to multiple occurrences with conflicting impacts as noted in the literature (Ahmad and Chen, 2020; Arnaud and Gourlay, 2012; Laborel-Préneron et al., 2017; Ratsimbazafy et al., 2021; Stevulova et al., 2013). Bamboo has a specific shape of particles where both its height and width are close in size, making it a good substitute for natural aggregates as in the case of the study by (Park et al., 2019). Nevertheless, lengthier particles could potentially lead to higher intermolecular porosity, resulting in poor mechanical performance (Ahmad and Chen, 2020; Benmahiddine et al., 2020; Laborel-Préneron et al., 2017; Niyigena et al., 2016; Stevulova et al., 2013; Williams et al., 2018). In contrast, lengthier rice straws resulted in relatively superior compressive strengths due to the chemical treatment (Morsy, 2011) has followed which aims to extract the pores of these particles. Moreover, (Arnaud and Gourlay, 2012) found that hemp concrete with ariel lime and larger shives enhanced CO2 diffusion, crucial for binder curing and hydration, thereby improving the mechanical effectiveness.

It is worth mentioning that for the same size of corn stalk aggregates, (Ahmad and Chen, 2020) found a compressive strength less than 2 MPa whereas (Ahmad et al., 2018) noted a compressive strength of up to 28 MPa. This enormous difference is due to the mechanical properties of the magnesium phosphate cement used by (Ahmad et al., 2018).

Chemical and physical interactions amid bio-aggregates and mineral binders have been studied (Bourdot et al., 2019; Diquélou et al., 2015; Sabathier et al., 2017). Generally, water-soluble contents from lignocellulosic aggregates disrupt the hydration process of the mineral binder at different ages (Diquélou et al., 2015; Magniont and Escadeillas, 2017). (Diquélou et al., 2015) used chemical FTIR analysis to show that water-soluble contents in hemp shives create a halo of unhydrated cement, reducing the creation of hydrates such as C-S-H and portlandite, thereby weakening the mechanical performance. Fig. 12 presents the compressive stress of sample cement pastes based on aggregate water-soluble content over 7 days. (Diquélou et al., 2015) established a correlation between delayed setting in three cement pastes, leached from three distinct hemp particles, and the compressive stress of the corresponding sample pastes. The compressive stress decreased as water-soluble mass content increased, with a 25% reduction in the worst case, attributed to few hydrates formed (C-S-H and portlandite). In a parallel study (Sabathier et al., 2017), also observed the same tendency in bio-based concrete with Portland cement and pozzolanic binder, using sunflower bark and lavender straw as aggregates. In both types of mineral binders used, water-soluble content of sunflower barks (SB) is less than lavender straws (LS), which means that sunflower barks have a mitigated effect on compressive strength. Indeed, for water soluble content of 10.6%, bio-based concrete with SB reached a compressive stress of 42.5 MPa and 24 MPa, for composites with Portland cement and pozzolanic binder, respectively (Sabathier et al., 2017). This compressive strength declined by 25% and 50% after one week, when lavender straws were employed (22.7% water soluble content) in the composition of plant-based specimens with Portland cement and pozzolanic cement, respectively. Conversely, the lignocellulosic extracts of sunflower barks and lavender straws did not significantly affect the compressive stress of lime-based composites, owing to ariel setting of lime and carbonation of $Ca(OH)_2$. In the same context, (Bourdot et al., 2019) found a very low compressive strength in corn bark composites due to substantial delay caused by water extractives on the heat flow of the pozzolanic paste, reaching up to 27 h of delay. These findings suggest a potential correlation between mechanical performance, water-soluble compound dosage, and nature in aggregates. Additionally, different binders' effects on plant-based concrete highlight the need to study components from

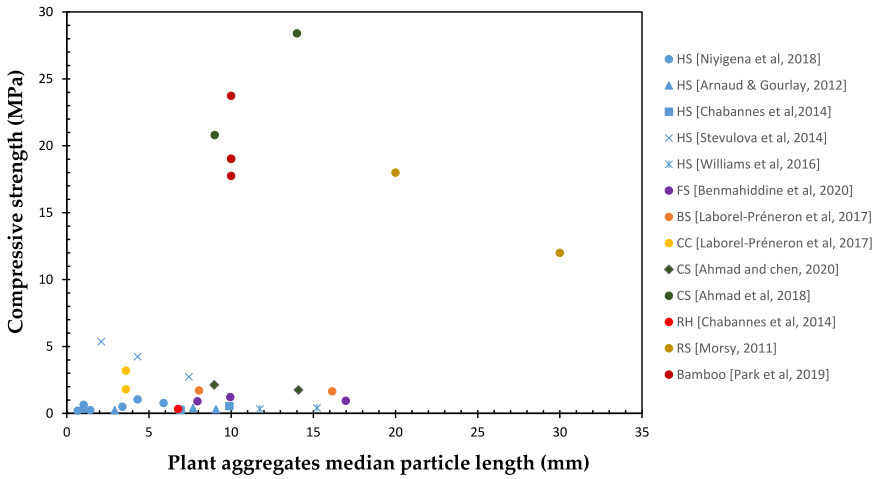

Fig. 11. Compressive strength of plant-based concrete and earth-based materials as a function of particle length across different studies (HS: hemp shives; FS: flax shives; BS: barely straw; CC: corn cob; CS: corn stalk; RH: rice husk (RS: rice straw; Bamboo).

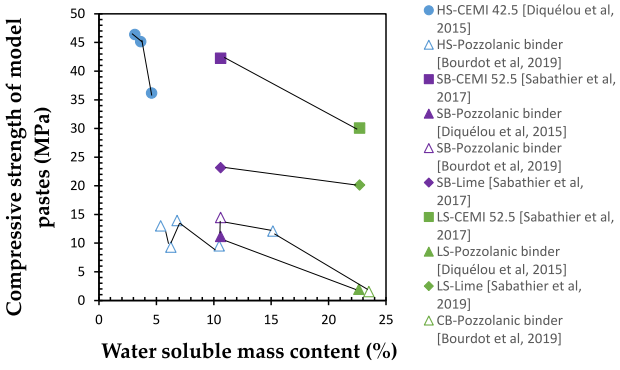

Fig. 12. Compressive strength of plant-based concrete with respect to water-soluble content across different studies (HS: hemp shives; SB: sunflower bark; LS: lavender straw; CB: corn bark) (Ratsimbazafy et al., 2021).

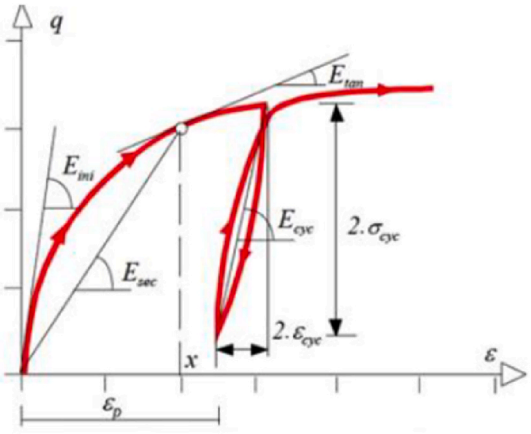

Fig. 13. Schematic representation of the various modulus during the compressive behavior of bio-based concrete (Borel and Reiffsteck, 2006).

basic extraction (pH 9 and 12) (Ratsimbazafy et al., 2021).

3.1.2. *Young's modulus*

The modulus values of bio-based concrete vary widely between the studies. This fluctuation arose from diverse factors such as the composition, formulation, casting process, storing conditions, and the methodology used for assessing this parameter. In the last case, (Niyigena et al., 2016, 2019) obtained an enormous variability in modulus values based on the assessing method. Young's modulus varies due to the pronounced non-linearity of the mechanical behavior of bio-based concrete even in the elastic phase (Niyigena et al., 2016). As of today, there is no conventional method or standard by which modulus is calculated (Niyigena et al., 2019). Plant-based concrete can have several types of modulus depending on the type of compression tests (Akkaoui et al., 2017; Mazhoud et al., 2017). For instance, 4 different types of moduli exist in cyclic compression tests: E_{ini} (apparatus modulus), E_{sec} (secant modulus), E_{cyc} (elastic modulus), E_{tan} (hardening modulus). However, for monotonic compression test, only the apparatus modulus can be calculated (Niyigena et al., 2016, 2019). These moduli are graphically schematized in Fig. 13. E_{ini} corresponds to the apparatus modulus, determined as the slope during the beginning of loading in the stress-strain curve; E_{sec} represents the slop at various loading levels which connects the origin into the tangent point; E_{cyc} is the modulus of elasticity which corresponds to the invertible slope at the recharging/loading cycles; E_{tan} corresponds to the setting modulus, computed at the completion of the initial loading phase. Three different approaches were used in assessing the modulus: Tangential, floating, and cyclic. Out of these approaches, the floating method emerged as the most suitable due to its minimal dispersion and consistent performance over time (Niyigena et al., 2019).

Fig. 14 illustrates Young's modulus values for the different bio-based concrete related to aggregate content. It must be noted that for the same aggregate content, different values of Young's modulus were registered due to varying sample densities as compaction energy increased, as observed in the following studies (Akkaoui et al., 2017; Brouard et al., 2018). Sunflower pith concrete stands as one of the least robust materials compared to other bio-based specimens with a Young's modulus ranging between 3 MPa and 6 MPa for an aggregate content of 17 % between varied densities (Brouard et al., 2018). This evidence was explained by (Brouard et al., 2017) due to the low binder/aggregate ratio for sunflower concrete which prohibited the binder skeleton from taking shape around the aggregates, leading to a sharp decrease in Young's modulus.

Hemp concrete (Hirst et al., 2010; Laborel-Préneron et al., 2017; Nguyen et al., 2010; Véronique, 2005), rice-husk concrete (Chabannes et al., 2015), and barely straw concrete (Giroudon et al., 2019; Laborel-Préneron et al., 2017) reached the same rigidity range as

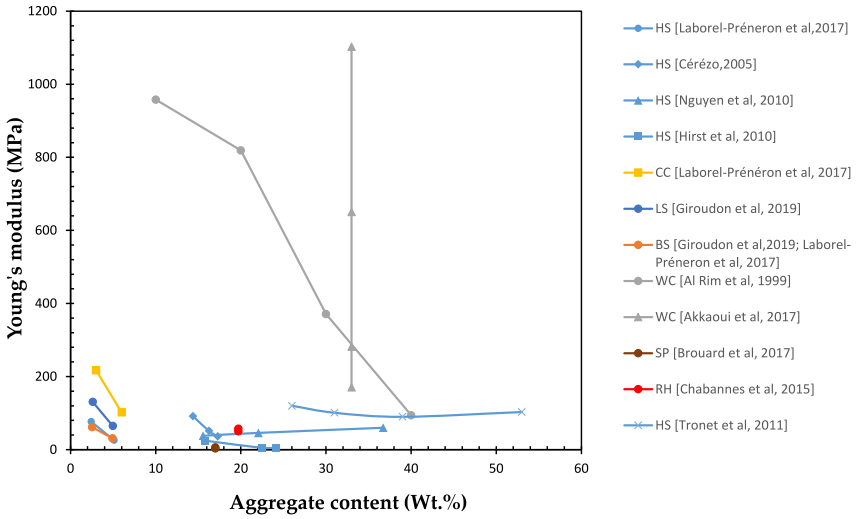

Fig. 14. Young's modulus of bio-based concrete and earth-based composites with respect to aggregate content across different studies (HS: hemp shives; CC: corn cob; BS: barely straw; LS: lavender straw; WC: wood chips; RH: rice husk; SP: sunflower pith).

between 20 MPa and 80 MPa regardless the variability of aggregate content. However, in the study of (Tronet et al., 2011), the high compactness of hemp shives up to 500 kg/m^3 led to relatively higher modulus values in the range of 100–120 MPa regardless of the high aggregate content exceeding 50 %. This evidence is in line with the fact that a high compaction load can stiffen the composite specimen by reducing the intermolecular voids even in the case of a high aggregate percentage.

Wood concrete is considered the most robust bio-based material with a rigidity reaching up to 980 MPa (Akkaoui et al., 2017) and 1100 MPa (Al Rim et al., 1999). This tremendous increase is due to the high density of wood concretes and the superior mechanical properties of wood chips compared to other aggregates.

A similar tendency to compressive stress can be remarked, where the rigidity of the plant-based concrete decreases as aggregate content increases. Indeed, (Mazhoud et al., 2017) noted a decrease in elastic modulus from 26.12 MPa to 16.25 MPa when the shives-to-binder ratio rise from 0.4 to 0.75, respectively, leading to a relationship between these two parameters as follow: Ec 12.878 × (hemp/binder)$^{-0.742}$. Furthermore, a linear relationship was found between Young's modulus and compressive stress. In the same regard, (Chamoin, 2013) found that compressive strength has a linear evolution closer to the increase of apparent modulus than elastic one. In contrast to aggregate content, the modulus increases when cement content increases. Some studies described this evidence by the ability of high cement content to fill intermolecular porosity (Akkaoui et al., 2017; Murphy et al., 2010). The type of bio-particles used has a significant impact on the rigidity of the plant-based specimens. For instance, for the same binder type and aggregate content, the rigidity of earth-based composites varied proportionally composites with hemp shives, lavender straws, and corn cobs (Laborel-Préneron et al., 2017). This can be linked to the bulk density of the aggregates and their physical characteristics. As a matter of fact, the size of the aggregate used can impact directly the Young's modulus. For instance, (Niyigena et al., 2016) found that smaller shives led to higher Young's modulus than composites with large shives. Similarly, (Arnaud and Gourlay, 2012) elaborated that smaller shives showed a better and more thorough mineral binder coating during the mixing process. Furthermore, the initial water absorption rate of smaller aggregates is less than large aggregates, where (Akkaoui et al., 2017) showed that the elastic properties (Young's modulus) of wood aggregates decreased from 12670 MPa to 10300 MPa between a water content of 12% and 25%, respectively.

3.2. Properties under flexural loading

3.2.1. Flexural strength

Flexural strength is a key parameter of plant-based concrete, indicating its ability to resist bending stress(Jami et al., 2019). Fig. 15 illustrates the flexural strength of various bio-based materials with respect to aggregate content. The differences of flexural strength for the same aggregate content as the case of hemp concrete tested by (Sassoni et al., 2014) are due to the variabilities in densities due to different compaction pressures. Unlike compressive strength, there's no direct relationship between bio-particles content and flexural stress. In fact, plant aggregates impact flexural and compressive strength differently. For instance, (Belhadj et al., 2016) showed that adding aggregates can increase flexural strength by up to 6 %, along with other improvements such as lightness, deformability, and ductility. However, after reaching a certain extent of aggregate proportions, further increases in aggregate content result in a drop in flexural strength. In contrast, the same authors found that increasing barley straw content resulted in declining compressive stress and increasing dimensional variations (Belhadj et al., 2016). In addition, (Agossou and Amziane, 2023) revealed that the flexural stress of flax gypsum composites increased from 1.46 kN to 3.42 kN by increasing fiber content from 1 to 3 %, respectively. Nevertheless, great variability of flexural strength occurred due to fiber length (Agossou and Amziane, 2023). Indeed, (Laborel-Préneron et al., 2017) observed that earth composites made with short barely straws demonstrated a higher flexural strength of 1.8 MPa, compared to 1.6 MPa for those made with long straws, due to density variations. This finding (Laborel-Préneron et al., 2017) contradicts those of (Danso et al., 2015; Mostafa and Uddin, 2015) who reported that longer fibers improve flexural strength by increasing adhesion area. (Laborel-Préneron et al., 2017) supported their findings with two reasons: short straw particles mixed more thoroughly with the matrix, leading to a better distribution of coated particles; and specimens with short barely straws had better visual surface quality, indicating improved adhesion and mechanical resistance. Some studies (Al Rim et al., 1999; Elfordy et al., 2008) established exponential and linear relationships between increasing density and increased flexural strength in plant-based concrete. Hereinafter, establishing a direct relationship between aggregate or fiber content and specimen density is crucial to understanding fluctuations in

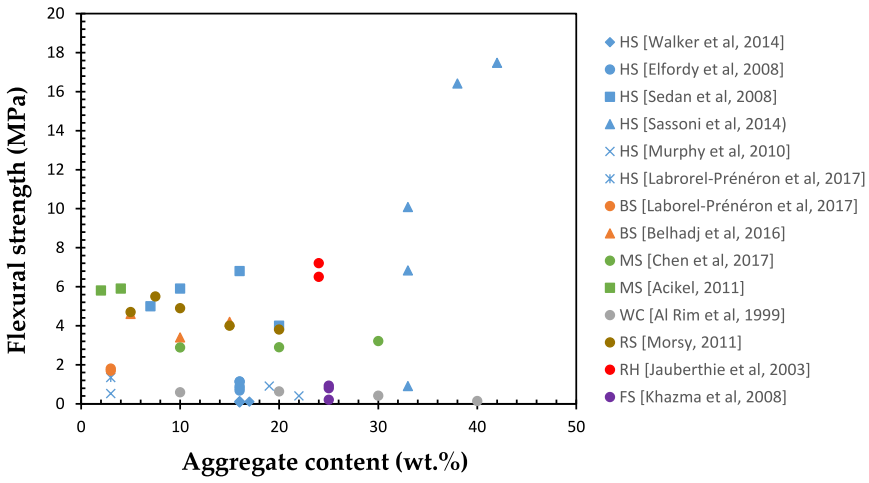

Fig. 15. Flexural strength of plant-based concrete and earth-based composites related to aggregate content across different studies (HS: hemp shives; BS: barely straw; MS: miscanthus stem, WC: wood chips; RS: rice straw; RH: rice husk; FS: flax shives).

flexural strength with varying fiber content. Although, most researches in the literature showed that adding bio-aggregates results in increasing the flexural strength (Agossou and Amziane, 2023; Al Rim et al., 1999; Aymerich et al., 2016; Bouhicha et al., 2005; Galán-Marín et al., 2010), only one study (Al Rim et al., 1999) investigated that flexural strength begins to decrease after the aggregate content exceeds 10 %. This decrease is due to two competing phenomena: the shape of wood aggregates, and the decrease in matrix's volume proportions (Al Rim et al., 1999). Furthermore, (Morsy, 2011) noted that the flexural stress of rice straw concrete increased up to 5.49 MPa for 7.5% of aggregate content, while additional increases in aggregate content resulted in a declined flexural stress. Other studies (Belhadj et al., 2016; Murphy et al., 2010; Sedan et al., 2008) reported the same findings. More particularly, (Murphy et al., 2010) observed that a lower load-carrying capacity was found for composites with higher aggregate content. This was evident as flexural strength showed an increase when binder content was risen by 25% and 50%, yet increasing this latter to 90% had a mitigated effect on the flexural stress of hemp concrete. Hence, the bond between hemp shives and lime significantly contributes to the composite's flexural strength.

(Belhadj et al., 2016) observed that barely straw concrete with a maximum flexural strength of 4.6 MPa, prevented the specimen's splitting after crack initiation due to the tensile properties of barely straw. (Chen et al., 2017) noted the same evidence for miscanthus aggregates, where the tensile strength of miscanthus fibers (180–260 MPa) mitigates the negative impact of high miscanthus content on flexural strength through crack bridging. (Sellami et al., 2013) found that horizontal fiber arrangement enhances tensile resistance and flexural strength.

For structural applications, standards must be met. In this regard, the Masonry Standards Joint Committee mandates minimum flexural stress of 0.21 MPa for clay and concrete blocks ("TMS 402/602-08 Building Code Requirements and Specification for Masonry Structures, 2008," n. d."BS 6073–1:1981 Precast concrete masonry units. Specification for precast concrete masonry units (AMD 3944) (AMD 4462) (Withdrawn), British Standards Institution - Publication Index | NBS," n.d.), while British Standard BS 6073 mandates at least 0.65 MPa for building materials("BS 6073–1:1981 Precast concrete masonry units. Specification for precast concrete masonry units (AMD 3944) (AMD 4462) (Withdrawn), British Standards Institution - Publication Index | NBS," n.d."BS 6073–1:1981 Precast concrete masonry units. Specification for precast concrete masonry units (AMD 3944) (AMD 4462) (Withdrawn), British Standards Institution - Publication Index | NBS," n.d.). Hemp concrete has been extensively studied for flexural properties, with Hempcrete Company LTD reporting a flexural stress in the range of 0.3–0.4 MPa (Abbott, 2014). Other studies report values from 0.11 to 0.15 MPa for hemp concrete (Elfordy et al., 2008; Murphy et al., 2010; Walker et al., 2014). A similar range of flexural strength was reported for other bio-based specimens with the following aggregates: flax shives (Khazma et al., 2008), and wood chips (Al Rim et al., 1999). Nevertheless, (Sassoni et al., 2014) found that hybrid binders (Канти, 2012) and varying nominal densities can affect the flexural strength of hemp concrete to a large extent. For instance, low-density composites achieved similar flexural strengths to those found by (Sedan et al., 2008), but medium and high-density composites had flexural strengths 17 times higher than typical values, making comparison difficult (Sassoni et al., 2014). (Sedan et al., 2008) reported high flexural strengths (4–7 MPa), due to superior mechanical properties of hemp fibers compared to shives. The discrepancy between studies arises from different testing norms, such as the French norm EN196-1 ("EN 196-1," n.d.) followed by these studies (Jauberthie et al., 2003; Walker et al., 2014; "EN12089 - Determination of bending behaviour of Thermal Insulation Products.," n.d.), the European standard EN 12089 ("EN12089 - Determination of bending behaviour of Thermal Insulation Products.," n.d."EN12089 - Determination of bending behaviour of Thermal Insulation Products.," n.d.) followed by Sassoni et al. (2014), and the French standards NF 18–407 ("NF P18-407," n.d.) used by (Al Rim et al., 1999).

3.2.2. *Flexural modulus*

Unlike Young's modulus, which is determined from the steady linear section of the compressive response of bio-based concrete, the flexural modulus is calculated using a mathematical equation. (Agossou and Amziane, 2023) provided the formula for determining the flexural modulus of plant-based mortars:

$$E_{elast} = \frac{0.21L^2}{bh^3}\left(\frac{\Delta F}{\Delta S}\right) \quad (1)$$

Where, 0.21 is an empirical constant as recommended by the Norm UNE EN ISO 14125 (Standards, n.d.); E_{elast} in MPa; L denotes the length of the specimen, in mm; b denotes the width, in mm; h denotes the thickness, in mm; ΔS denotes the change in deflection; ΔF denotes load between, in N;

Fig. 16 shows that flexural modulus decreases as aggregate or fiber content increases in plant-based concrete and mortars. This reduction in stiffness is attributed to increased porosity caused by higher aggregate content (Agossou and Amziane, 2023; Iucolano et al., 2015, 2018). (Le

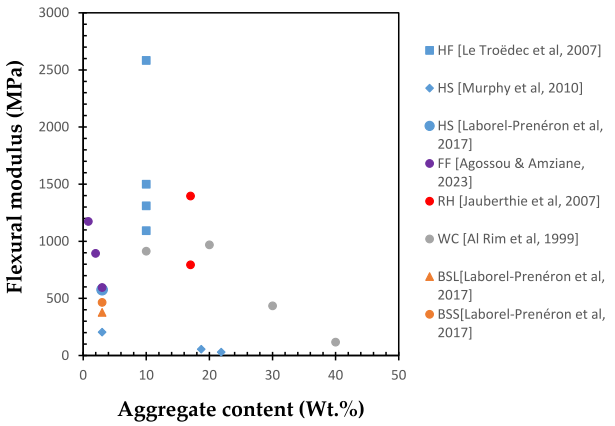

Fig. 16. Flexural modulus of plant-based composites across different studies (HF: hemp fiber; HS: hemp shives; BSS: barely straw short; BSL: barely straw long; FF: flax fiber; RH: rice husk; WC: wood chips).

Troedec et al., 2007) reported very high values of flexural modulus, which can be explained by special treatments applied on hemp fibers, as the flexural modulus of 10% hemp mortars increased from 1090 MPa for untreated hemp fibers to 2590 MPa for NaOH-treated fibers.

3.3. Properties under shear loading

3.3.1. Deviatoric shear stress

Fig. 17 illustrates the mean peak deviatoric stress q for various confining lateral pressures (ranging from 25 kPa to 150 kPa). Two key mechanical parameters, the maximum friction angle (φ_p) and the bonding or cohesion (C), were derived from failure lines of plant-based concrete using linear analysis of the maximum values, as defined by equations (2) and (3), respectively. Fig. 18 (a) illustrates the forces diagram in the case of a triaxial shear test.

$$\varphi = \arcsin \frac{3M'}{M' + 6} \tag{2}$$

$$C = C(\psi) \times \frac{Sin_{\varphi}}{M'} \tag{3}$$

M' is the ratio of deviatoric stress to mean effective pressure and relates to the gradient of the failure trajectory in q-σ_m' diagram as shown in Fig. 18 (b) (M' = q/σ_m'). (Youssef et al., 2015) found M' hard to determine due to the continuous ascending shear behavior, preventing

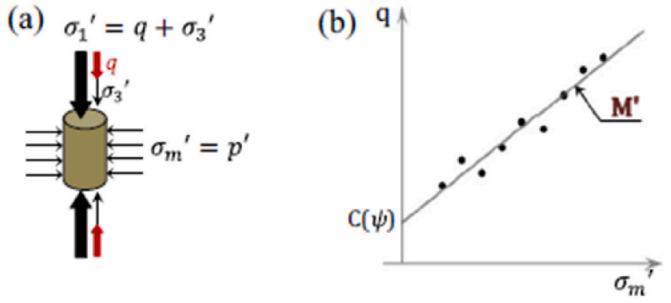

Fig. 18. (a): State of stress during triaxial compression test, (b): Coordinates of failure trajectory q-σ_m' (Chabannes et al., 2017).

the identification of a peak deviatoric stress. Generally, the deviatoric stress was higher for lime-hemp concrete than rice husk concrete across all confining pressures. This is attributed to the difference in friction angle 46° for lime-hemp concrete compared to 29° for rice husk concrete, although both had similar cohesion of approximately 0.36 MPa. Based on the models applied for traditional concrete (Zingg et al., 2016), as well as to sand and clays strengthened or by cement injection (Horpibulsuk, 2005; Maalej et al., 2007), the friction angle was commonly associated with the granular skeleton (interlocking in bio-aggregates), while the bonding among aggregates (C) predominantly contributed to cohesion. The higher friction angle of lime-hemp concrete can be explained by the shives size range which provides better packing of the particles and shear strength. Additionally, the morphological characteristics of the aggregates such as particle shape (thin semi-ellipsoidal for husk versus thick parallelepiped for shives), surface roughness, and rigidity are all inherent features that impact the friction angle.

3.3.2. Shear modulus

Fig. 19 shows the shear Young's modulus for two types of bio-based concrete with respect to the lateral confining pressure. The shear Young's modulus was very dependent on the failure patterns of the specimens. Indeed, lime-hemp concrete specimens experiencing FM1 failure mode exhibited higher modulus compared to those with FM1/2 or FM2 failure modes. For instance, at a lateral confining pressure of 150 kPa, the shear Young's modulus for lime-rice husk (LRC) decreased from 260 MPa under FM1 (shear banding) to 220 MPa under FM2 (bulging). An intermediate modulus was observed for the combined failure mode (FM1/2). The results indicate that for non-uniform density specimens (FM2 failure mode), the modulus corresponds to the weaker part with a higher void ratio. However, within the same failure mode,

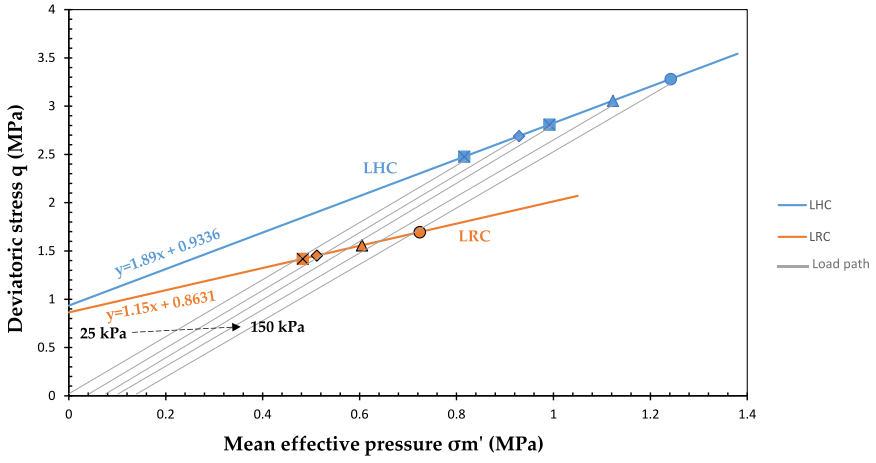

Fig. 17. Shear strength of bio-based concrete with respect to confining pressure (Chabannes et al., 2017).

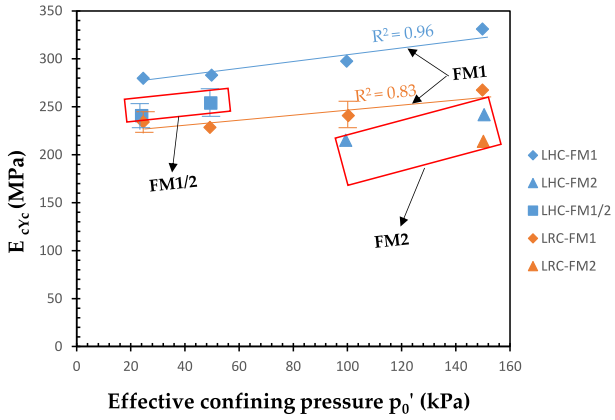

Fig. 19. Relationship between shear modulus and lateral confining pressure (Chabannes et al., 2017).

the modulus varied linearly with the confining pressure, similar to granular materials (Becquart, 2006). The authors noted that LHC specimens had a higher shear modulus than LRC specimens, aligning with a weaker mechanical behavior under unconfined compression for LRC (Chabannes et al., 2017).

4. Factors affecting the mechanical properties of bio-based building materials

4.1. Formulation

The formulation of bio-based concrete can be considered one of the major factors influencing its mechanical performance, particularly its fresh density and subsequent compressive strength. Fig. 20 illustrates the compressive stress of lime-hemp concrete with distinct formulations, all measured at 28 days of curing (Arnaud and Gourlay, 2012; Chabannes et al., 2014; Dinh, 2014; Mukherjee and MacDougall, 2013; Nguyen et al., 2010; Tronet et al., 2016) except for one study (Gross and Walker, 2014) which measured strength after 5 months. The data shows that a higher binder-to-aggregate (B/A) ratio generally results in a rise in compressive stress. However, the tremendous rise in the compressive stress at a low B/A ratio of 0.5 in the study of (Tronet et al., 2016) is attributed to the substantial impact of compaction energy. As a matter of fact, the compressive stress values listed in the following studies(Dinh, 2014; Mukherjee and MacDougall, 2013; Nguyen et al., 2010; Tronet et al., 2016) were relatively higher than previous mechanical investigations on hemp-lime concrete due to enhanced compaction energy during the casting process.

4.1.1. Binder content

The binder content tremendously affects the mechanical response and properties of bio-based concrete, with higher binder content generally indicating a low aggregate content, and vice versa. According to some studies (Arnaud and Gourlay, 2012; Véronique, 2005), increasing the binder content, enhances the mechanical characteristics of bio-based concrete, resulting in a higher peak. (Véronique, 2005) identified three distinct mechanical behaviors of hemp concrete based on the binder content as illustrated in Fig. 21. For low binder content, the composites exhibit better ductility with particles linked by rigid "bridges of binder. Similarly, (Arnaud and Gourlay, 2012) observed a long plateau of ductility in low binder content, attributing it to the significant role of hemp particles when the binder quantity is insufficient. With intermediate content of binder, the bio-based specimen consists of aggregates enveloped by hydrate layers of different thicknesses. However, the high content of binder results in aggregates being buried inside a continuous binder matrix, which predominantly determines the mechanical characteristics of bio-based concrete. Two hypotheses arise from (Véronique, 2005): Firstly, higher binder content makes plant-based concrete more similar to mineral binder in terms of brittleness and higher mechanical properties; Secondly, lower binder content indicates higher aggregate proportions, leading to a better ductility but lower mechanical properties due to increased porosity. (Murphy et al., 2010) reported similar findings (Fig. 22), noting a more brittle and pronounced compressive behavior with increased commercial lime binder up to 90%, while lower binder content (10%) resulted in better strain at failure but lower mechanical loading. Additionally, a higher binder content expands the elastic zone at the initial phase (Murphy et al., 2010; Véronique, 2005), as explained by (Akkaoui et al., 2017) because the mineral matrix primarily carries the load during the elastic phase. Nevertheless, (Nguyen et al., 2009, 2010) presented different observations regarding binders. Irrespective of hemp concrete bulk density and water/binder ratio, they found that compressive strength increased at 7.5% of strain with higher aggregate content. This can be explained by the compaction energy applied by the authors as higher compactness was performed for composites with higher aggregate content. In contrast to previous studies, (Akkaoui et al., 2017;

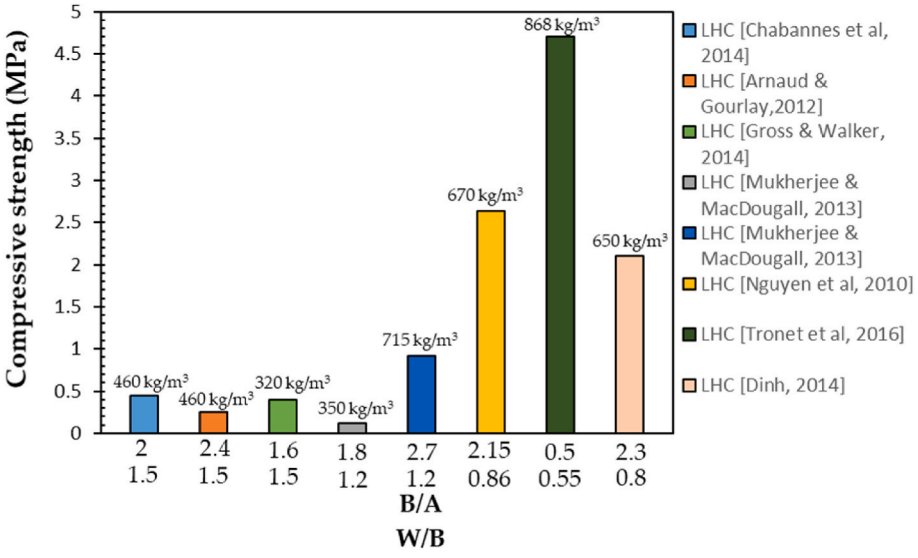

Fig. 20. Effect of mix formulation on the compressive stress of hemp-lime concrete(B/A: binder/aggregate; W/B: water/binder).

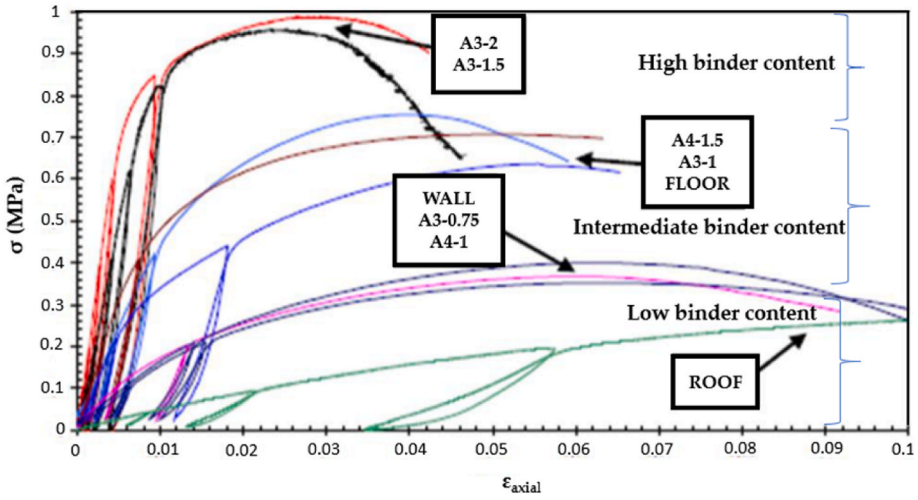

Fig. 21. Effect of binder content on the mechanical behavior of hemp concrete (Véronique, 2005).

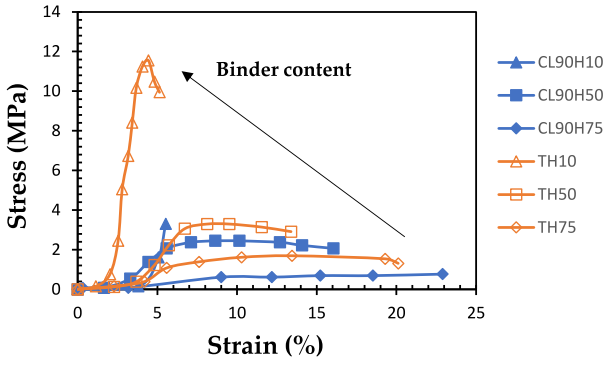

Fig. 22. Influence of two distinct binders content on the mechanical behavior of hemp concrete (Murphy et al., 2010).

Murphy et al., 2010; Véronique, 2005; Nguyen et al., 2009) obtained a lower strain at maximum stress for configurations with higher binder content regarding low compactness bio-based composites.

4.1.2. Aggregate content

A proportional relationship exists between high aggregate content and decreased mechanical properties. (Bouguerra et al., 1998a) found that increased wood proportions significantly raise the porosity of the wood-concrete. These higher micropores leads to lighter apparent density, which in turns results in lower mechanical properties (Elfordy et al., 2008). Similar discussions were elaborated in section 3.1.1 of this review.

4.2. Aggregates characteristics

4.2.1. Aggregate size

The size of the aggregate significantly impacts the intermolecular porosity and mechanical properties of bio-based concrete. (Niyigena et al., 2018) discussed that large particles resulted in weak binding between the bio-based composite constituents, leading to low mechanical properties. Similar findings were observed by (Benmahiddine et al., 2020) with flax concrete, where larger aggregates produced lower compressive strength compared to smaller ones. Additionally, elongated aggregates tend to retain more water, leading to a dry mixture and further reducing mechanical properties (Niyigena et al., 2016, 2018). Conversely, plant-based composites made with smaller and finer aggregates exhibited better mechanical performance (Arnaud and Gourlay, 2012; Niyigena, 2016). Indeed, (Niyigena et al., 2018) noted an increase in bulk density for hempcrete with smaller particle size. Similarly, (Chen et al., 2017) showed that a finer aggregate, achieved through grinding, improves the apparent density and mechanical performance of miscanthus concrete. (Arnaud and Gourlay, 2012) explained that finer aggregates slow down CO_2 diffusion, decelerating hardening kinetics and enhancing mechanical properties. Moreover, a better coating of small aggregates with mineral binder was found to enhance the mechanical properties of bio-based composite (Arnaud and Gourlay, 2012; Niyigena et al., 2016).

The size of particles alters the mechanical behavior of plant-based concrete. For instance, (Niyigena et al., 2018) identified three distinct behaviors based on aggregate size: low strain (around 3% at σ_{max}), medium strain (around 5% at σ_{max}), and high strain (beyond 20%). Hence, for optimized mechanical properties, finer and smaller aggregates are recommended (Arnaud and Gourlay, 2012).

4.3. Binder characteristics

4.3.1. Effect of nature of binder

Several mineral binders were employed in the formulation of plant-based concrete, including lime-based binder (Arnaud and Gourlay, 2012; Véronique, 2005), pozzolanic binders (Sinka et al., 2014; Walker et al., 2014), Mgo based binder (Ahmad et al., 2018; Sassoni et al., 2014), Portland cement (de Bruijn et al., 2009; Sassu et al., 2016), pre-formulated lime binder (Arnaud and Gourlay, 2012; Nguyen et al., 2009, 2010), and prompt natural cement (Niyigena et al., 2016). Some of these binders have been approved and made available for utilization alongside hemp shives, such as: NHL2 (Pavier's white lime), NHL 3.5 (Saint Astier's pure white lime), NHL 3.5 Z: (Lafarge's white lime), and tradical pre-mixed binder PF 70 (Amziane and Arnaud, 2013; Arnaud and Gourlay, 2012). As a matter of fact, (Arnaud and Gourlay, 2012) conducted an experimental study to evaluate the effect of these validated mineral binders on the mechanical response of hemp concrete. Fig. 23 (a) illustrates the mechanical behavior of hemp concrete having the exact formulations and cured at the same conditions but with different mineral binders. The compressive stress of hemp concrete with NHL 3.5 reached 0.15 MPa, whereas this parameter reached a maximum of 0.32 MPa when PF 70 was employed. A similar enhancement in rigidity can be noticed for PF 70 mineral binder. This can be explained by the composition of PF 70 mineral binder, whose pozzolanic proportions enhance its setting and hydration mechanisms. In a parallel study, (Lagouin et al., 2019) examined the influence of mineral binders on sunflower bark and maize concrete. Fig. 23 (b) demonstrates that metakaolin-sunflower concrete exhibits higher mechanical strength

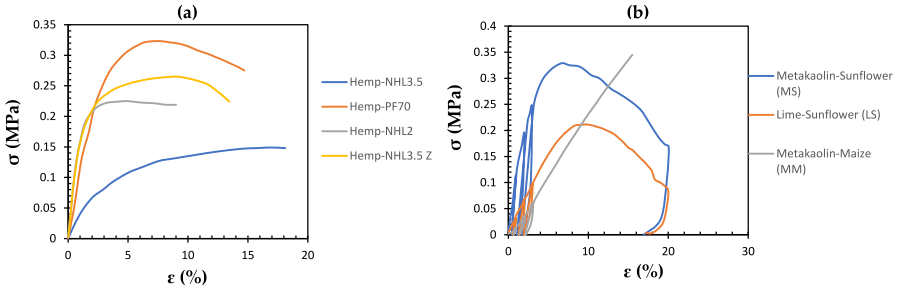

Fig. 23. Effect of mineral binder type on the mechanical behavior of bio-based concrete, (a): (Arnaud and Gourlay, 2012), (b) (Lagouin et al., 2019):

than lime-sunflower concrete. The evidence was attributed to the mechanical response between lime-based pre-mixed binder and metakaolin-pozzolanic based binder paste alone. More particularly, the mechanical strength of mortars made with lime, and modified by pozzolan additions, demonstrated an improvement due to shrinkage decrease, which minimizes cracking around aggregates in mortars (Nežerka et al., 2014).

4.4. Casting process

4.4.1. Effect of initial compactness

The compaction pressure applied during casting significantly influences the mechanical properties of bio-based concrete. It must be noted that the pressure exerted by the top plunger or punch of the compaction device during the casting process of (Nguyen, 2010; Nguyen et al., 2009, 2010) and in previous studies (Arnaud and Gourlay, 2012; Bouloc, 2006; de Bruijn et al., 2009; Elfordy et al., 2008; Evrard et al., 2008; Jalali et al., 2006; "Utilisation du chanvre pour la préfabrication d'éléments de construction - ProQuest," n.d.) was never higher than 2.5 MPa.

Fig. 24(a) and (b) illustrates a nomenclature and schematical representation of the compaction devices used in the following studies (Nguyen et al., 2009, 2010; Tronet et al., 2016). In the literature, the following studies have assessed the effect of compaction energy on the mechanical properties of bio-based concrete (Nguyen et al., 2009, 2010; Tronet et al., 2011, 2016). In general, the compactness pressure is proportional to the apparent density of plant-based concrete, which diminishes the volume of void spaces or intergranular pores at the microstructure of the bio-based concrete (Nguyen et al., 2009). They showed in Fig. 24 (c) that for the same binder/aggregate ratio, a heavier compaction led to a more pronounced mechanical behavior and so to better mechanical properties. Hence, the compressive stress of plant-based concrete is directly correlated to the compaction stress applied during casting (Nguyen et al., 2010; Tronet et al., 2016). In a parallel study, (Tronet et al., 2011) obtained the highest value of compressive strength for lime-hemp concrete reported in the literature owing to the compaction process applied to bulk mixtures. The authors revealed a value of 7 MPa for compressive strength at 7.5% of strain.

4.5. Curing conditions

The curing conditions play an essential role in predicting the mechanical properties of bio-based concrete since they alter the humidity of the environment in which the hydrates of the mineral binder will be formed. Different studies have evaluated the influence of curing conditions on the mechanical properties of bio-based concrete (Arnaud and Gourlay, 2012; Jauberthie et al., 2003). For example, (Arnaud and Gourlay, 2012) cured hemp concrete samples at 20 °C placed in various relative humidity conditions: 30%, 50%, 75%, and 98%. Fig. 25 displays

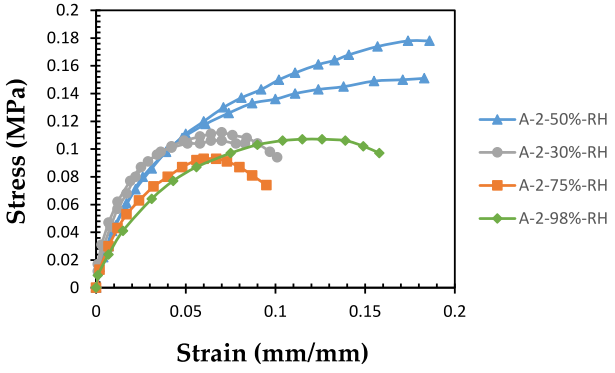

Fig. 25. Effect of storage conditions under various relative humidity (RH) on the mechanical behavior of hemp concrete (Arnaud and Gourlay, 2012).

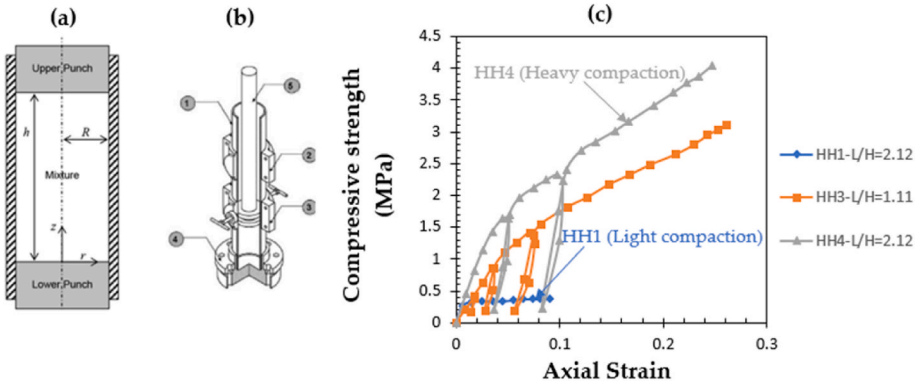

Fig. 24. Compaction devices utilized in (a):(Tronet et al., 2016), (b):(Nguyen et al., 2009), (c): Mechanical behavior of hemp concrete made with different degrees of compactness (Nguyen et al., 2009).

the mechanical behavior of the same hemp concrete under various curing conditions. It is evident that with severe humidity levels (98% RH), the mechanical properties of hemp concrete tend to deteriorate. Indeed, moist conditions significantly decelerate the setting process of hemp concrete. They attributed this evidence to the atmospheric curing of a binder (Arnaud and Gourlay, 2012). Typically, the passage of CO_2 from the atmosphere into the voids or the pores of a lime mortar is obstructed when the internal moisture level of the material is exceptionally high (Van Balen and Van Gemert, 1994). This is due to the saturation of mortar's pores prioritizes transfers in the liquid phase, which occur far more slowly than in the gas phase in a full saturated setting. (Arnaud and Gourlay, 2012) provided another argument to support the very low mechanical properties in case of high moisture content (RH of 75% and 98%), related to the physical and chemical interactions between shives and binder that disrupt the mechanical setting of hemp concrete. The same consequences were remarked in poor humid conditions (30% RH) where a severe slowdown in the curing of hydraulic lime-based binder occurred. However, (Jauberthie et al., 2003) have shown that compressive strength was higher in humid conditions (95% RH) than in normal conditions (50% RH). The authors explained that high humidity conditions (95% RH), were suitably conductive to pozzolanic reactivity than medium humidity (50% RH) (Jauberthie et al., 2003). In contrast, flexural strength decreased from 7.2 MPa at 50% RH to 6.5 MPa at 95% RH. The contradiction found between compressive and flexural stress is actually related to the impact of storing conditions on fiber content. For instance, a decrease in the degree of fiber reinforcement occurred from 3.66 at 95% RH to 2.86 at 50% RH between compression and flexural loading, respectively (Jauberthie et al., 2003).

4.6. Physico-chemical interactions between particles and binder

The water-soluble compounds of lignocellulosic aggregate can adversely affect the curing and setting of the mineral binder, thereby influencing the mechanical properties of the whole composite (Bourdot et al., 2019; Diquélou et al., 2015; Sabathier et al., 2017). In fact, the extracts of aggregates (sugar, protein, phenolic compounds, ash, and others) induce a delay on the setting and hydration mechanisms of plant-based concrete (Diquélou et al., 2015). Indeed, (Delhomme et al., 2022) have shown a complete formation of a hallo covering a few millimeters at the interfacial transition zone between aggregate and cement paste after 12 h of age as seen in Fig. 26 (a). The same findings of a non-hydrated hallo area around aggregates were recorded by (Diquélou et al., 2015) as seen in Fig. 26 (b). According to (Diquélou et al., 2015), this few millimeters halo area has a significant impact on the limited distance between particles (size of interparticle matrix), and a notable effect on the amount of cement included in a traditional bio-based concrete. As a consequence, the aggregates extracts act as a strong retarding agent which reduces the quantityt of hydrates formed (C-S-H and portlandite), resulting in lower mechanical properties). (Delhomme et al., 2022) performed an FTIR mapping to illustrate the change in area under the portlandite band wavenumber. The code of colors of mapping in Fig. 26 (c) ranges from blue indicating a very small area of vibration, though green, to red highlighting a larger area of vibration. The color transition ranged from green to red, indicating varying levels of portlandite concentration from the least concentrated area (ITZ or non-hydrated zone) to the most concentrated area (hydrated zone) as schematized in Fig. 26 (d).

5. Application of bio-based concrete

Bio-based concrete began to be applied in walls, slabs and plasters in the early 90's in France (Allin, 2005; Magwood, 2016). Their applications consists mainly of timber frame walls (Barbhuiya and Bhusan Das, 2022; Wadi et al., 2023), roofing insulation panels (Magwood, 2016; Sassoni et al., 2014), floor, rendering, new construction and repair works (Kawaai et al., 2022; Tziviloglou et al., 2016). Depending on each type of application, 3 main parameters are usually tailored to meet the desirable criteria's: formulation, mechanical strength, and rigidity (Amziane and Arnaud, 2013; Vo and Navard, 2016). For instance, the minimum threshold mechanical performance that must be respected for hemp concrete regarding the following applications: walls (compressive strength and elasticity modulus higher than 0.2 and 15 MPa, respectively); roofs (compressive strength and elasticity modulus higher than 0.05 and 3 MPa, respectively); floors (compressive strength and elasticity modulus higher than 0.3 and 15 MPa, respectively); rendering (elasticity modulus higher than 20 MPa); flagging (compressive strength and elasticity modulus higher than 0.3 and 20 MPa, respectively) (Amziane and Arnaud, 2013). Accordingly, most of hemp concrete specimens evaluated in this review can meet the standards for these types of application as shown in Figs. 10 and 14, respectively. Taking into account that hemp concrete is among the least mechanical performant bio-based materials as elaborated in Figs. 10 and 14, other bio-based materials can endure a more pronounced load application up to some extent of aggregates dosage. Furthermore, formulation alters the use of bio-based specimens depending on 3 levels of binder dosage: low, intermediate, and high (Amziane and Arnaud, 2013; Véronique, 2005). For instance, for the same type of binder (Tradical PF 70), the formulations in terms of mass percentage for roofs (25.1% hemp shive, 24.6 % binder, 50.3% water), walls (16.5 % hemp shive, 33.7 % binder, 49.8% water), and floors (14.2% hemp shive, 34.8 % binder, 50.9 % water) (Véronique, 2005). It can be noticed that the binder content increases progressively from low content for roofs to high content for floors. This is in accordance with the mechanical requirements of each application as previously noted which implies higher binder content for application that requires superior mechanical performance. It must be noted that the formulation of any bio-based concrete regarding its application depends to large extent on the density of the binder and the water absorption of the aggregates.

To this end, bio-based concrete especially hemp concrete was used as

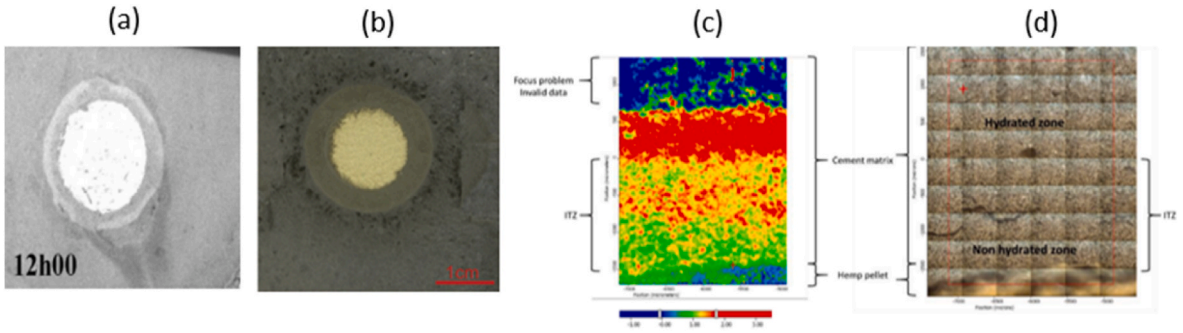

Fig. 26. Halo zone formation around the grain, (a):(Delhomme et al., 2022), (b): (Diquélou et al., 2015), (c): Infrared mapping, (d) The observed region of the vibration band area corresponding to Portlandite (3640 cm^{-1}) (Delhomme et al., 2022).

tamped infill materials in timber frame walls (Wadi et al., 2023), and pre-cast blocks which cover several range of thermal and mechanical benefits (Collet and Pretot, 2014; Jami et al., 2019). Moreover, hemp shives play an efficient role in wall rendering and floor screed applications since it reduces the quantity of binder, promotes the structural integrity of the binder by securing a bonding interface between the surface and the render (Jami et al., 2019). Rendering can be applied on hemp concrete after a recommended period between 3 and 10 weeks, with a preferable natural hydraulic lime since it allows faster hardening, lower pigmentation, and less microbial colonization (Arizzi et al., 2018).

Hemp concrete walls can be cast in situ, which is common, or they can be precast into blocks off-site and assembled on-site using conventional masonry techniques (Sáez-Pérez et al., 2020). Fig. 27 depicts two buildings with load-bearing hemp walls: one constructed with prefabricated hemp concrete blocks (A) and the other with cast, compacted hemp concrete (B). Additionally, it includes building blocks made from hemp concrete mixed with either a clay binder (C) or NHL3.5 lime (D). Images (E) and (F) illustrate a non-loadbearing building featuring an internal timber structure and cast, non-rendered hemp-lime concrete walls. Likewise, Fig. 28 illustrates a hemp-based house built in Florida, USA.

Other bio-based specimens like miscanthus concrete, corn stalk concrete, and rice straw concrete can be used as load-bearing blocks for an aggregate content of 5% or less thanks to their superior mechanical strength as shown in Fig. 10. In this regard, Fig. 29 presents the different stage of using miscanthus concrete from isolation panels to an entire house built with them. The proportions of miscanthus during the casting process has a critical influence on the potential use of these materials whether for insulation or structural applications. Moreover, a refining process of aggregates promotes the mechanical performance of these bio-based materials and so their application.

Fig. 28. Hemp-based house built in Florida, USA ("Hempcrete House," n.d.).

In addition, bio-based materials were often used as self-healing materials that target the recovery and repair of existing ordinary concrete by regaining water tightness lost by cracking (Tziviloglou et al., 2016). In fact, the bacteria presented in bio-based materials became active when a crack bridged in a hardened concrete, which in case precipitate limestone and seal the open crack. In the same context,

Fig. 27. Hemp concrete constructions can be created using pre-made building blocks (A) or by casting and compacting load-bearing hemp-clay concrete walls (B). These building blocks are made from hemp shives (2–25 mm) combined with either a clay binder (C) or a lime binder, with the optional addition of mineral pigments (D). Images (E) and (F) depict various views of a building constructed with non-load-bearing, cast hemp-lime concrete walls after 20 years of exposure to weather conditions in Switzerland. (G) illustrates the sprayed application of hemp concrete as an exterior coating(Sáez-Pérez et al., 2020).

Fig. 29. (a): Miscanthus-based mix and block (author's work), (b): miscanthus based noise barrier and (c): a house built with miscanthus concrete in Louvain-la-Neuve, Belgium("D.Robinet, les utilisations du miscanthus, 2009," n.d.).

theoretical explanations suggest that electro-chemical reactions account for the enhancement of corrosion resistance in ordinary concrete can be due to the consumption of dissolved oxygen by bacteria, which may act as a cathodic inhibitor (Kawaai et al., 2022).

Therefore, it is evident that bio-based materials can be effectively used to build eco-friendly buildings that ensure both optimal thermal/acoustic comfort and positive environmental impact.

6. Conclusions

Drawing from the gathered data in the literature about the mechanical behavior of bio-based concrete under various loadings (compressive, flexural, and shear), and the factors affecting the mechanical properties of these materials, the following points can be concluded.

- **Mechanical Behavior:** Bio-based concrete exhibits similar compressive and shear responses, described by an elastoplastic behavior with three distinct phases: linear, plateau, and failure, while flexural response consists of a linear phase followed by progressive failure as the load transfers to the aggregates.
- **Deformability:** Bio-based concrete shows significant deformability across different loading types (compression, flexural, shear), especially for specimens with high aggregate content oriented orthogonally to compaction, making it effective for energy dissipation in seismic events.
- **Compressive Strength:** Hemp concrete has compressive strength ranging from 0.1 to 2 MPa, with higher values (up to 7 MPa) under compaction pressure. Similar ranges were found in concretes with flax shives, wood chips, and other plant-based aggregates. Strength is higher in concretes using miscanthus, corn stalk, and rice straw, making them viable load-bearing materials when properly refined and chemically treated.
- **Young's Modulus:** Bio-based concretes containing hemp, flax, barley, and rice husks have a Young's modulus below 200 MPa, while wood, sunflower, and corn cob concretes exhibit relatively higher modulus values.
- **Flexural Strength**: Most bio-based concretes have flexural strength between 1 and 6 MPa, with compaction processes increasing strength up to 17 MPa.
- **Shear Strength:** Hemp-lime concrete exhibits higher peak shear strength (3.2 MPa) than rice-husk concrete (1.5 MPa), attributed to hemp's better particle arrangement and reduced voids.
- **Binder and Aggregate Content:** High binder content/low aggregate content increases mechanical performance but reduces ductility, and vice-versa. Optimum mechanical performance is obtained at an aggregate content of less than 10 %.
- **Water-Soluble Extracts:** Increased water-soluble extracts generally decrease compressive strength, with hemp having the least impact and corn cob the most severe. The effect varies by aggregate and binder type.
- **Aggregate Size:** Smaller aggregates enhance mechanical properties due to better bonding and lower water absorption, while longer aggregates offer higher deformability.

CRediT authorship contribution statement

Rafik Bardouh: Writing – review & editing, Writing – original draft, Methodology, Investigation, Formal analysis, Conceptualization. **Evelyne Toussaint:** Writing – review & editing, Validation, Supervision, Methodology, Investigation. **Sofiane Amziane:** Writing – review & editing, Validation, Supervision, Resources, Project administration, Formal analysis. **Sandrine Marceau:** Writing – review & editing, Visualization, Supervision, Project administration, Methodology.

Declaration of competing interest

The authors declare that they have no known competing financial interests or personal relationships that could have appeared to influence the work reported in this paper.

Acknowledgements

The authors wish to extend their appreciation to the French National Research Agency (ANR) with Partnership of VICAT for funding the BIOUP project (ANR-21-CE22-0009) on which this study took part.

Data availability

Data will be made available on request.

References

Abbas, M.S., McGregor, F., Fabbri, A., Ferroukhi, M.Y., 2020. The use of pith in the formulation of lightweight bio-based composites: impact on mechanical and hygrothermal properties. Construct. Build. Mater. 259, 120573. https://doi.org/10.1016/j.conbuildmat.2020.120573.

Abbott, T., 2014. Hempcrete factsheet - essential hempcrete info [WWW Document]. Limecrete Co. URL. https://limecrete.co.uk/hempcrete-factsheet/. accessed 1.24.24.

Acikel, H., 2011. The Use of Miscanthus (Giganteus) as a Plant Fiber in Concrete Production.

Agossou, O.G., Amziane, S., 2023. Analysis of mechanical and thermal performance and environmental impact of flax-fiber-reinforced gypsum boards. Buildings 13, 3098. https://doi.org/10.3390/buildings13123098.

Agricultural Waste Materials as Thermal Insulation for TH, [WWW Document], n.d. . pdfcoffee.com. URL https://pdfcoffee.com/agricultural-waste-materials-as-thermal-insulation-for-th-pdf-free.html (accessed 1.26.24).

Ahmad, M.R., Chen, B., 2020. Influence of type of binder and size of plant aggregate on the hygrothermal properties of bio-concrete. Construct. Build. Mater. 251, 118981. https://doi.org/10.1016/j.conbuildmat.2020.118981.

Ahmad, M.R., Chen, B., Haque, M.A., Saleem Kazmi, S.M., Munir, M.J., 2021. Development of plant-concrete composites containing pretreated corn stalk bio-aggregates and different type of binders. Cem. Concr. Compos. 121, 104054. https://doi.org/10.1016/j.cemconcomp.2021.104054.

Ahmad, M.R., Chen, B., Yousefi Oderji, S., Mohsan, M., 2018. Development of a new bio-composite for building insulation and structural purpose using corn stalk and magnesium phosphate cement. Energy Build. 173, 719–733. https://doi.org/10.1016/j.enbuild.2018.06.007.

Akkaoui, A., Caré, S., Vandamme, M., 2017. Experimental and micromechanical analysis of the elastic properties of wood-aggregate concrete. Construct. Build. Mater. 134, 346–357. https://doi.org/10.1016/j.conbuildmat.2016.12.084.

Al Rim, K., Ledhem, A., Douzane, O., Dheilly, R.M., Queneudec, M., 1999. Influence of the proportion of wood on the thermal and mechanical performances of clay-cement-wood composites. Cem. Concr. Compos. 21, 269–276. https://doi.org/10.1016/S0958-9465(99)00008-6.

Allin, S., 2005. Building with Hemp. SeedPress.

Amziane, S., Collet, F., 2017. Bio-aggregates Based Building Materials: State-Of-The-Art Report of the RILEM Technical Committee 236-BBM. Springer.

Arizzi, A., Brümmer, M., Martín-Sánchez, I., Molina, E., Cultrone, G., 2018. Optimization of lime and clay-based hemp-concrete wall formulations for a successful lime rendering. Construct. Build. Mater. 184, 76–86. https://doi.org/10.1016/j.conbuildmat.2018.06.225.

Arnaud, L., Gourlay, E., 2012. Experimental study of parameters influencing mechanical properties of hemp concretes. Construct. Build. Mater. 28, 50–56. https://doi.org/10.1016/j.conbuildmat.2011.07.052.

Asasutjarit, C., Hirunlabh, J., Khedari, J., Charoenvai, S., Zeghmati, B., Shin, U.C., 2007. Development of coconut coir-based lightweight cement board. Construct. Build. Mater. 21, 277–288. https://doi.org/10.1016/j.conbuildmat.2005.08.028.

Aymerich, F., Fenu, L., Francesconi, L., Meloni, P., 2016. Fracture behaviour of a fibre reinforced earthen material under static and impact flexural loading. Construct. Build. Mater. 109, 109–119. https://doi.org/10.1016/j.conbuildmat.2016.01.046.

Bakkour, A., Ouldboukhitine, S.-E., Biwole, P., Amziane, S., 2024. A review of multi-scale hygrothermal characteristics of plant-based building materials. Construct. Build. Mater. 412, 134850. https://doi.org/10.1016/j.conbuildmat.2023.134850.

Barbhuiya, S., Bhusan Das, B., 2022. A comprehensive review on the use of hemp in concrete. Construct. Build. Mater. 341. https://doi.org/10.1016/j.conbuildmat.2022.127857.

Becquart, F., 2006. Caractérisation du comportement mécanique d'un mâchefer dans la perspective d'une méthodologie de dimensionnement adaptée aux structures de chaussées.

Belhadj, B., Bederina, M., Makhloufi, Z., Dheilly, R.M., Montrelay, N., Quéneudéc, M., 2016. Contribution to the development of a sand concrete lightened by the addition of barley straws. Construct. Build. Mater. 113, 513–522. https://doi.org/10.1016/j.conbuildmat.2016.03.067.

Benitha Sandrine, U., Isabelle, V., Ton Hoang, M., Chadi, M., 2015. Influence of chemical modification on hemp–starch concrete. Construct. Build. Mater. 81, 208–215. https://doi.org/10.1016/j.conbuildmat.2015.02.045.

Benmahiddine, F., Cherif, R., Bennai, F., Belarbi, R., Tahakourt, A., Abahri, K., 2020. Effect of flax shives content and size on the hygrothermal and mechanical properties of flax concrete. Construct. Build. Mater. 262, 120077. https://doi.org/10.1016/j.conbuildmat.2020.120077.

Borel, S., Reiffsteck, P., 2006. Caractérisation de la déformabilité des sols au moyen d'essais en place. In: Etudes et recherches des Laboratoires des ponts et chaussées. Série Géotechnique. Presented at the Caractérisation de la déformabilité des sols au moyen d'essais en place.

Bouasker, M., Belayachi, N., Hoxha, D., Al-Mukhtar, M., 2014. Physical characterization of natural straw fibers as aggregates for construction materials applications. Materials 7, 3034–3048. https://doi.org/10.3390/ma7043034.

Bouguerra, A., Ledhem, A., de Barquin, F., Dheilly, R.M., Quéneudec, M., 1998a. Effect of microstructure on the mechanical and thermal properties of lightweight concrete prepared from clay, cement, and wood aggregates. Cement Concr. Res. 28, 1179–1190. https://doi.org/10.1016/S0008-8846(98)00075-1.

Bouguerra, A., Ledhem, A., Laurent, J.P., Diop, M.B., Queneudec, M., 1998b. Thermal effusivity of two-phase wood cement-based composites. J. Phys. Appl. Phys. 31, 2184. https://doi.org/10.1088/0022-3727/31/17/017.

Bouhicha, M., Aouissi, F., Kenai, S., 2005. Performance of composite soil reinforced with barley straw. Cem. Concr. Compos., Natural fibre reinforced cement composites 27, 617–621. https://doi.org/10.1016/j.cemconcomp.2004.09.013.

Bouloc, P., 2006. Le chanvre industriel: production et utilisations. France Agricole Editions.

Bourdot, A., Magniont, C., Lagouin, M., Niyigena, C., Evon, P., Amziane, S., 2019. Impact of bio-aggregates properties on the chemical interactions with mineral binder, application to vegetal concrete. J. Adv. Concr. Technol. 17, 542–558. https://doi.org/10.3151/jact.17.542.

Boutin, M.P., Flamin, C., Quinton, S., Gosse, G., 2006. Etude des caractéristiques environnementales du chanvre par l'analyse de son cycle de vie. Ministère L'agriculture Pêche Fr 102.

Brouard, Y., Belayachi, N., Hoxha, D., Méo, S., Abdallah, W., 2017. Hygrothermal behavior of clay - sunflower (helianthus annuus) and rape straw (Brassica napus) plaster bio-composites for building insulation. Adv. Eng. Forum 21, 242–248. https://doi.org/10.4028/www.scientific.net/AEF.21.242.

Brouard, Y., Belayachi, N., Hoxha, D., Ranganathan, N., Méo, S., 2018. Mechanical and hygrothermal behavior of clay – sunflower (Helianthus annuus) and rape straw (Brassica napus) plaster bio-composites for building insulation. Construct. Build. Mater. 161, 196–207. https://doi.org/10.1016/j.conbuildmat.2017.11.140.

Amziane, S., Arnaud, L., 2013. Bio-aggregate-based Building Materials: Applications to Hemp Concretes | Wiley [WWW Document]. Wiley.com. URL https://www.wiley.com/en-br/Bio+aggregate+based+Building+Materials%3A+Applications+to+Hemp+Concretes-p-9781848214040 (accessed 12.15.23).

BS 6073-1:1981 Precast concrete masonry units. Specification for precast concrete masonry units (AMD 3944) (AMD 4462) (Withdrawn), British Standards Institution - Publication Index | NBS [WWW Document], n.d. URL https://www.thenbs.com/PublicationIndex/documents/details?Pub=BSI&DocID=11651 (accessed 1.24.24).

Chabannes, M., Becquart, F., Garcia-Diaz, E., Abriak, N.-E., Clerc, L., 2017. Experimental investigation of the shear behaviour of hemp and rice husk-based concretes using triaxial compression. Construct. Build. Mater. 143, 621–632. https://doi.org/10.1016/j.conbuildmat.2017.03.148.

Chabannes, M., Bénézet, J.-C., Clerc, L., Garcia-Diaz, E., 2014. Use of raw rice husk as natural aggregate in a lightweight insulating concrete: an innovative application. Construct. Build. Mater. 70, 428–438. https://doi.org/10.1016/j.conbuildmat.2014.07.025.

Chabannes, M., Garcia-Diaz, E., Clerc, L., Bénézet, J.-C., 2015. Studying the hardening and mechanical performances of rice husk and hemp-based building materials cured under natural and accelerated carbonation. Construct. Build. Mater. 94, 105–115. https://doi.org/10.1016/j.conbuildmat.2015.06.032.

Chamoin, J., 2013. Optimisation des propriétés (physiques, mécaniques et hydriques) de bétons de chanvre par la maîtrise de la formulation.

Chen, Y., Yu, Q.L., Brouwers, H.J.H., 2017. Acoustic performance and microstructural analysis of bio-based lightweight concrete containing miscanthus. Construct. Build. Mater. 157, 839–851. https://doi.org/10.1016/j.conbuildmat.2017.09.161.

Collet, F., Pretot, S., 2014. Experimental highlight of hygrothermal phenomena in hemp concrete wall. Build. Environ. 82, 459–466. https://doi.org/10.1016/j.buildenv.2014.09.018.

Collet, F., Pretot, S., Mazhoud, B., Bessette, L., Lanos, C., 2015. Comparing hemp composites made with mineral or organic binder on thermal, hygric and mechanical point of view. Acad. J. Civ. Eng. 33, 228–234. https://doi.org/10.26168/icbbm2015.35.

Construire en chanvre. Règles professionnelles d'éxécution - SEBTP, (n.d).

Corrêa, A.A.R., Mendes, L.M., Barbosa, N.P., Protásio, T. de P., Campos, N. de A., Tonoli, G.H.D., 2015. Incorporation of bamboo particles and "synthetic termite saliva" in adobes. Construct. Build. Mater. 98, 250–256. https://doi.org/10.1016/j.conbuildmat.2015.06.009.

Costantine, G., Harb, E., Bliard, C., Maalouf, C., Kinab, E., Abbès, B., Beaumont, F., Polidori, G., 2020. Experimental characterization of starch/beet-pulp bricks for building applications: drying kinetics and mechanical behavior. Construct. Build. Mater. 264, 120270. https://doi.org/10.1016/j.conbuildmat.2020.120270.

Cuenca, J., Rodríguez, J., Martín-Morales, M., Sánchez-Roldán, Z., Zamorano, M., 2013. Effects of olive residue biomass fly ash as filler in self-compacting concrete. Constr. Build. Mater., Special Section on Recycling Wastes for Use as Construction Materials 40, 702–709. https://doi.org/10.1016/j.conbuildmat.2012.09.101.

Dalmay, P., Smith, A., Chotard, T., Sahay-Turner, P., Gloaguen, V., Krausz, P., 2010. Properties of cellulosic fibre reinforced plaster: influence of hemp or flax fibres on the properties of set gypsum. J. Mater. Sci. 45, 793–803. https://doi.org/10.1007/s10853-009-4002-x.

Danso, H., Martinson, D.B., Ali, M., Williams, J., 2015. Effect of fibre aspect ratio on mechanical properties of soil building blocks. Construct. Build. Mater. 83, 314–319. https://doi.org/10.1016/j.conbuildmat.2015.03.039.

de Bruijn, P.B., Jeppsson, K.-H., Sandin, K., Nilsson, C., 2009. Mechanical properties of lime–hemp concrete containing shives and fibres. Biosyst. Eng. 103, 474–479. https://doi.org/10.1016/j.biosystemseng.2009.02.005.

Delhomme, F., Prud'homme, E., Julliot, C., Guillot, T., Amziane, S., Marceau, S., 2022. Effect of hemp on cement hydration: experimental characterization of the interfacial transition zone. Results Chem 4, 100440. https://doi.org/10.1016/j.rechem.2022.100440.

Dinh, T.M., 2014. Contribution au développement de béton de chanvre préfabriqué utilisant un liant pouzzolanique innovant, vol. 3. These de doctorat), Toulouse.

Diquélou, Y., Gourlay, E., Arnaud, L., Kurek, B., 2015. Impact of hemp shiv on cement setting and hardening: influence of the extracted components from the aggregates and study of the interfaces with the inorganic matrix. Cem. Concr. Compos. 55, 112–121. https://doi.org/10.1016/j.cemconcomp.2014.09.004.

de Bruijn, P., 2008. Hemp Concretes: mechanical properties using both shives and fibers.

D. Robinet, les utilisations du miscanthus, 2009, (n.d).

Elfordy, S., Lucas, F., Tancret, F., Scudeller, Y., Goudet, L., 2008. Mechanical and thermal properties of lime and hemp concrete ("hempcrete") manufactured by a projection process. Construct. Build. Mater. 22, 2116–2123. https://doi.org/10.1016/j.conbuildmat.2007.07.016.

EN 196-1. 2016 - methods of testing cement - Part 1: determination of strength. https://standards.iteh.ai/catalog/standards/cen/37b8816e-4085-4dcc-a642-a383d9bddd6c/en-196-1-2016 accessed 1.12.24.

EN12089 - Determination of bending behaviour of Thermal Insulation Products [WWW Document]. https://www.instron.com/en/testing-solutions/other-standards/en-12089. accessed 1.12.24.

Evrard, A., Pritchett, I., Mawditt, I., 2008. Hemp Lime Construction – A Guide to Building with Hemp Lime Composites, pp. 63–69.

Galán-Marín, C., Rivera-Gómez, C., Petric, J., 2010. Clay-based composite stabilized with natural polymer and fibre. Construct. Build. Mater. 24, 1462–1468. https://doi.org/10.1016/j.conbuildmat.2010.01.008.

Garikapati, K.P., Sadeghian, P., 2020. Mechanical behavior of flax-lime concrete blocks made of waste flax shives and lime binder reinforced with jute fabric. J. Build. Eng. 29, 101187. https://doi.org/10.1016/j.jobe.2020.101187.

Ghavami, K., Toledo Filho, R.D., Barbosa, N.P., 1999. Behaviour of composite soil reinforced with natural fibres. Cem. Concr. Compos. 21, 39–48. https://doi.org/10.1016/S0958-9465(98)00033-X.

Giroudon, M., Laborel-Préneron, A., Aubert, J.-E., Magniont, C., 2019. Comparison of barley and lavender straws as bioaggregates in earth bricks. Construct. Build. Mater. 202, 254–265. https://doi.org/10.1016/j.conbuildmat.2018.12.126.

Glouannec, P., Collet, F., Lanos, C., Mounanga, P., Pierre, T., Poullain, P., Pretot, S., Chamoin, J., Zaknoune, A., 2011. Propriétés physiques de bétons de chanvre. Mater. Technol. 99, 657–665. https://doi.org/10.1051/mattech/2011047.

Gross, C., Walker, P., 2014. Racking performance of timber studwork and hemp-lime walling. Construct. Build. Mater. 66, 429–435. https://doi.org/10.1016/j.conbuildmat.2014.05.054.
Hempcrete House. https://hempcretehouse.coffeecup.com/ accessed 9.20.24.
Hirst, E.A., Walker, P., Paine, K.A., Yates, T., 2010. Characterisation of Low Density Hemp-Lime Composite Building Materials under Compression Loading.
Hirth, G., Tullis, J., 1989. The effects of pressure and porosity on the micromechanics of the brittle-ductile transition in quartzite. J. Geophys. Res. Solid Earth 94, 17825–17838. https://doi.org/10.1029/JB094iB12p17825.
Horpibulsuk, S., 2005. Mechanism controlling undrained shear characteristics of induced cemented clays. Lowland Technol. Int. 7, 9–18.
Huang, G., Abou-Chakra, A., Absi, J., Geoffroy, S., 2022. Optimization of mechanical properties in anisotropic bio-based building materials by a multiscale homogenization model. J. Build. Eng. 57, 104890. https://doi.org/10.1016/j.jobe.2022.104890.
Iucolano, F., Caputo, D., Leboffe, F., Liguori, B., 2015. Mechanical behavior of plaster reinforced with abaca fibers. Construct. Build. Mater. 99, 184–191. https://doi.org/10.1016/j.conbuildmat.2015.09.020.
Iucolano, F., Liguori, B., Aprea, P., Caputo, D., 2018. Evaluation of bio-degummed hemp fibers as reinforcement in gypsum plaster. Composites, Part B 138, 149–156. https://doi.org/10.1016/j.compositesb.2017.11.037.
Jalali, S., Camões, A., Eires, R., Nunes, P., 2006. New Eco-Friendly Hybrid Composite Materials for Civil Construction.
Jami, T., Karade, S.R., Singh, L.P., 2019. A review of the properties of hemp concrete for green building applications. J. Clean. Prod. 239, 117852. https://doi.org/10.1016/j.jclepro.2019.117852.
Jauberthie, R., Rendell, F., Tamba, S., Cissé, I.K., 2003. Properties of cement—rice husk mixture. Construct. Build. Mater. 17, 239–243. https://doi.org/10.1016/S0950-0618(03)00005-9.
Kawaai, K., Nishida, T., Saito, A., Hayashi, T., 2022. Application of bio-based materials to crack and patch repair methods in concrete. Construct. Build. Mater. 340, 127718. https://doi.org/10.1016/j.conbuildmat.2022.127718.
Khazma, M., El Hajj, N., Goullieux, A., Dheilly, R.M., Queneudec, M., 2008. Influence of sucrose addition on the performance of a lignocellulosic composite with a cementious matrix. Composer Part Appl. Sci. Manuf. 39, 1901–1908. https://doi.org/10.1016/j.compositesa.2008.09.014.
kioy, S., 2005. Lime-hemp composites: compressive strength and resistance to fungal attacks. In: Bevan rand Woollet, T. (Ed.), Hemp Lime Construction, A Guide to Building with Hemp Lime Composites. https://scholar.google.com/scholar_lookup?title=Lime-Hemp. %20Composites%3A%20Compressive%20Strength%20and%20Resistance%20to%20Fungal%20Attacks&author=S.%20Kioy&publication_year=2005 (accessed 1.16.24).
Kristombu Baduge, S., Mendis, P., San Nicolas, R., Nguyen, K., Hajimohammadi, A., 2019. Performance of lightweight hemp concrete with alkali-activated cenosphere binders exposed to elevated temperature. Construct. Build. Mater. 224, 158–172. https://doi.org/10.1016/j.conbuildmat.2019.07.069.
Laborel-Préneron, A., Aubert, J.-E., Magniont, C., Maillard, P., Poirier, C., 2017. Effect of plant aggregates on mechanical properties of earth bricks. J. Mater. Civ. Eng. 29, 04017244. https://doi.org/10.1061/(ASCE)MT.1943-5533.0002096.
Laborel-Préneron, A., Magniont, C., Aubert, J.-E., 2018. Characterization of barley straw, hemp shiv and corn cob as resources for bioaggregate based building materials. Waste Biomass Valorization 9, 1095–1112. https://doi.org/10.1007/s12649-017-9895-z.
Lagouin, M., Magniont, C., Sénéchal, P., Moonen, P., Aubert, J.-E., Laborel-préneron, A., 2019. Influence of types of binder and plant aggregates on hygrothermal and mechanical properties of vegetal concretes. Construct. Build. Mater. 222, 852–871. https://doi.org/10.1016/j.conbuildmat.2019.06.004.
Lam, L., Teng, J.G., 2009. Stress–strain model for FRP-confined concrete under cyclic axial compression. Eng. Struct. 31, 308–321. https://doi.org/10.1016/j.engstruct.2008.08.014.
Le Troedec, M., Peyratout, C., Chotard, T., Bonnet, J.P., Smith, A., Guinebretiere, R., 2007. Physico-chemical modifications of the interactions between hemp fibres and a lime mineral matrix: impacts on mechanical properties of mortars. In: Heinrich, J.G., A, G. (Eds.), 10th International Conference of the European Ceramic Society, CD-Rom -. Göller Verlag, Berlin, Germany, pp. 451–456. ISBN 3-87264-022-4.
Lecompte, T., Tronet, P., Picandet, V., Baley, C., 2015. Study of lime and hemp concrete (LHC) – mix design, casting process and mechanical behaviors. Acad. J. Civ. Eng. 33, 281–288. https://doi.org/10.26168/icbbm2015.43.
Lertwattanaruk, P., Suntijitto, A., 2015. Properties of natural fiber cement materials containing coconut coir and oil palm fibers for residential building applications. Construct. Build. Mater. 94, 664–669. https://doi.org/10.1016/j.conbuildmat.2015.07.154.
Maalej, Y., Dormieux, L., Canou, J., Dupla, J.C., 2007. Strength of a granular medium reinforced by cement grouting. Compt. Rendus Mec. 335, 87–92. https://doi.org/10.1016/j.crme.2006.12.003.
Magniont, C., 2010. Contribution à la formulation et à la caractérisation d'un écomatériau de construction à base d'agroressources, vol. 3. These de doctorat, Toulouse.
Magniont, C., Escadeillas, G., 2017. Chemical composition of bio-aggregates and their interactions with mineral binders. In: Amziane, S., Collet, F. (Eds.), Bio-Aggregates Based Building Materials : State-Of-The-Art Report of the RILEM Technical Committee 236-BBM, RILEM State-Of-The-Art Reports. Springer, Netherlands, Dordrecht, pp. 1–37. https://doi.org/10.1007/978-94-024-1031-0_1.
Magniont, C., Escadeillas, G., Coutand, M., Oms-Multon, C., 2012. Use of plant aggregates in building ecomaterials. Eur. J. Environ. Civ. Eng. 16, s17–s33. https://doi.org/10.1080/19648189.2012.682452.
Magwood, C., 2016. Essential Hempcrete Construction: the Complete Step-by-step Guide. New Society Publishers.
Marri, A., 2010. The Mechanical Behaviour of Cemented Granular Materials at High Pressures.
Mazhoud, B., Collet, F., Pretot, S., Lanos, C., 2017. Mechanical properties of hemp-clay and hemp stabilized clay composites. Construct. Build. Mater. 155, 1126–1137. https://doi.org/10.1016/j.conbuildmat.2017.08.121.
Merzoud, M., 2011. Comportement mécanique et hydrique des composites à matrice cimentaire et argileuse à base de diss «Ampelodesma mauritanica.
Morsy, M.I.N., 2011. Properties of Rice Straw Cementitious Composite (Ph.D. Thesis). Technische Universität, Darmstadt.
Mostafa, M., Uddin, N., 2015. Effect of banana fibers on the compressive and flexural strength of compressed earth blocks. Buildings 5, 282–296. https://doi.org/10.3390/buildings5010282.
Mukherjee, A., MacDougall, C., 2013. Structural benefits of hempcrete infill in timber stud walls. Int. J. Sustain. Build. Technol. Urban Dev. 4, 295–305. https://doi.org/10.1080/2093761X.2013.834280.
Nežerka, V., Slížková, Z., Tesárek, P., Plachý, T., Frankeová, D., Petráňová, V., 2014. Comprehensive study on mechanical properties of lime-based pastes with additions of metakaolin and brick dust. Cement Concr. Res. 64, 17–29. https://doi.org/10.1016/j.cemconres.2014.06.006.
Murphy, F., Pavia, S., Walker, R., 2010. AN ASSESSMENT OF THE PHYSICAL PROPERTIES OF LIME-HEMP CONCRETE.
NF P18-407 [WWW Document], n.d. . Afnor Ed. URL https://www.boutique.afnor.org/fr-fr/norme/nf-p18407/betons-essai-de-flexion/fa016610/54905 (accessed 1.26.24).
Nguyen, T.T., 2010. Contribution à l'étude de la formulation et du procédé de fabrication d'éléments de construction en béton de chanvre (phdthesis). Université de Bretagne Sud, 10/document.
Nguyen, T.-T., Picandet, V., Amziane, S., Baley, C., 2009. Influence of compactness and hemp hurd characteristics on the mechanical properties of lime and hemp concrete. Eur. J. Environ. Civ. Eng. 13, 1039–1050. https://doi.org/10.1080/19648189.2009.9693171.
Nguyen, T.T., Picandet, V., Carre, P., Lecompte, T., Amziane, S., Baley, C., 2010. Effect of compaction on mechanical and thermal properties of hemp concrete. Eur. J. Environ. Civ. Eng. 14, 545–560. https://doi.org/10.1080/19648189.2010.9693246.
Niyigena, C., 2016. Variabilité des performances de bétons de chanvre en fonction des caractéristiques de la chènevotte produite en Auvergne (phdthesis). Université Blaise Pascal, Clermont-Ferrand II.
Niyigena, C., Amziane, S., Chateauneuf, A., 2019. Assessing the impact of calculation methods on the variability of Young's modulus for hemp concrete material. Construct. Build. Mater. 198, 332–344. https://doi.org/10.1016/j.conbuildmat.2018.11.174.
Niyigena, C., Amziane, S., Chateauneuf, A., 2018. Multicriteria analysis demonstrating the impact of shiv on the properties of hemp concrete. Construct. Build. Mater. 160, 211–222. https://doi.org/10.1016/j.conbuildmat.2017.11.026.
Niyigena, C., Amziane, S., Chateauneuf, A., Arnaud, L., Bessette, L., Collet, F., Lanos, C., Escadeillas, G., Lawrence, M., Magniont, C., Marceau, S., Pavia, S., Peter, U., Picandet, V., Sonebi, M., Walker, P., 2016. Variability of the mechanical properties of hemp concrete. Mater. Today Commun. 7, 122–133. https://doi.org/10.1016/j.mtcomm.2016.03.003.
Nozahic, V., Amziane, S., 2012. Influence of sunflower aggregates surface treatments on physical properties and adhesion with a mineral binder. Composer Part Appl. Sci. Manuf. 43, 1837–1849. https://doi.org/10.1016/j.compositesa.2012.07.011.
Nozahic, V., Amziane, S., Torrent, G., Saïdi, K., De Baynast, H., 2012. Design of green concrete made of plant-derived aggregates and a pumice–lime binder. Cem. Concr. Compos. 34, 231–241. https://doi.org/10.1016/j.cemconcomp.2011.09.002.
Park, S.-S., Hou, Y., Lee, J.-C., Jeong, S.-W., 2019. Mechanical properties of concrete with bamboo chips. Appl. Sci. 9, 3367. https://doi.org/10.3390/app9163367.
Pavia, S., Walker, R., McGinn, J., 2015. Effect of testing variables on the hydration and compressive strength of lime hemp concrete. Acad. J. Civ. Eng. 33, 635–640. https://doi.org/10.26168/icbbm2015.98.
Ratsimbazafy, H.H., Laborel-Préneron, A., Magniont, C., Evon, P., 2021. A review of the multi-physical characteristics of plant aggregates and their effects on the properties of plant-based concrete. Recent Prog. Mater. 3, 69.
Sabathier, V., Louvel, S., Correa, G., Magniont, C., Evon, P., Labonne, L., 2017. Incidence of the water-soluble compounds contained into lavender and sunflower bioaggregates on the hardening process of mineral binders. Acad. J. Civ. Eng. 35, 62–68. https://doi.org/10.26168/icbbm2017.7.
Sáez-Pérez, M.P., Brümmer, M., Durán-Suárez, J.A., 2020. A review of the factors affecting the properties and performance of hemp aggregate concretes. J. Build. Eng. 31, 101323. https://doi.org/10.1016/j.jobe.2020.101323.
Sassoni, E., Manzi, S., Motori, A., Montecchi, M., Canti, M., 2014. Novel sustainable hemp-based composites for application in the building industry: physical, thermal and mechanical characterization. Energy Build. 77, 219–226. https://doi.org/10.1016/j.enbuild.2014.03.033.
Sassu, M., Giresini, L., Bonannini, E., Puppio, M.L., 2016. On the use of vibro-compressed units with bio-natural aggregate. Buildings 6, 40. https://doi.org/10.3390/buildings6030040.
Sedan, D., Pagnoux, C., Smith, A., Chotard, T., 2008. Mechanical properties of hemp fibre reinforced cement: influence of the fibre/matrix interaction. J. Eur. Ceram. Soc. 28, 183–192. https://doi.org/10.1016/j.jeurceramsoc.2007.05.019.
Sellami, A., Merzoud, M., Amziane, S., 2013. Improvement of mechanical properties of green concrete by treatment of the vegetals fibers. Construct. Build. Mater. 47, 1117–1124. https://doi.org/10.1016/j.conbuildmat.2013.05.073.
Sheridan, J., Sonebi, M., Taylor, S., Amziane, S., 2017. Effect of viscosity modifying agent on the mechanical and transport properties of hemp and rapeseed straw

concrete. In: Sofiane AMZIANE, M.S. (Ed.), ICBBM 2017, 2nd International Conference on Bio-Based Building Materials, ICBBM 2017, Proceedings of the 2nd International Conference on Bio-Based Building Materials. RILEM, Clermont Ferrand, France.
Sinka, M., Radina, L., Sahmenko, G., Korjakins, A., Bajare, D., 2015. Enhancement of lime-hemp concrete properties using different manufacturing technologies. Acad. J. Civ. Eng. 33, 301–308. https://doi.org/10.26168/icbbm2015.46.
Sinka, M., Sahmenko, G., Korjakins, A., 2014. Mechanical properties of pre-compressed hemp-lime concrete. J. Sustain. Architect. Civ. Eng. 8, 92–99. https://doi.org/10.5755/j01.sace.8.3.7451.
Standards, E., n.d. UNE EN ISO 14125:1999 FIBRE-REINFORCED PLASTICS COMPOSITES. DETERMINATION OF FLEXURAL PROPERTIES (ISO 14125:1998) [WWW Document]. Httpswwwen-Stand. URL https://www.en-standard.eu/une-en-iso-14125-1999-fibre-reinforced-plastics-composites-determination-of-flexural-properties-iso-14125-1998/(accessed 9.20.24).
Stevulova, N., Kidalova, L., Cigasova, J., Junak, J., Sicakova, A., Terpakova, E., 2013. Lightweight composites containing hemp hurds. Procedia Eng., CONCRETE AND CONCRETE STRUCTURES 2013 - 6th International Conference, Slovakia 65, 69–74. https://doi.org/10.1016/j.proeng.2013.09.013.
Stevulova, N., Kidalova, L., Junak, J., Cigasova, J., Terpakova, E., 2012. Effect of hemp shive sizes on mechanical properties of lightweight fibrous composites. Procedia Eng., CHISA 42, 496–500. https://doi.org/10.1016/j.proeng.2012.07.441, 2012.
Sutton, A., Black, D., Walker, P., 2011. An Introduction to Low-Impact Building Materials.
Tancret, F., Osterstock, F., 2003. Indentation behaviour of porous materials: application to the Vickers indentation cracking of ceramics. Philos. Mag. A 83, 125–136. https://doi.org/10.1080/0141861021000013796.
Thomas, B.S., Yang, J., Mo, K.H., Abdalla, J.A., Hawileh, R.A., Ariyachandra, E., 2021. Biomass ashes from agricultural wastes as supplementary cementitious materials or aggregate replacement in cement/geopolymer concrete: a comprehensive review. J. Build. Eng. 40, 102332. https://doi.org/10.1016/j.jobe.2021.102332.
TMS 402/602-08 Building Code Requirements and Specification for Masonry Structures, 2008. Mason. Soc. URL n.d. https://masonrysociety.org/product/tms-0402-08/. accessed 1.24.24.
Transition to Sustainable Buildings: Strategies and Opportunities to 2050 | en | OECD n.d. URL https://www.oecd.org/publications/transition-to-sustainable-buildings-9789264202955-en.htm (accessed 6.June.23).
Tronet, P., Lecompte, T., Picandet, V., Baley, C., 2016. Study of lime hemp concrete (LHC) – mix design, casting process and mechanical behaviour. Cem. Concr. Compos. 67, 60–72. https://doi.org/10.1016/j.cemconcomp.2015.12.004.
Tronet, P., Picandet, V., Lecompte, T., Baley, C., 2011. Béton de chanvre : Effet du dosage en granulat sur les propriétés thermique et mécanique. In: AMAC (Ed.), 17èmes Journées Nationales Sur Les Composites (JNC17). Poitiers-Futuroscope, France, p. 161.
Tziviloglou, E., Van Tittelboom, K., Palin, D., Wang, J., Sierra-Beltrán, M.G., Erşan, Y.Ç., Mors, R., Wiktor, V., Jonkers, H.M., Schlangen, E., De Belie, N., 2016. Bio-based self-healing concrete: from research to field application. In: Hager, M.D., van der Zwaag, S., Schubert, U.S. (Eds.), Self-Healing Materials. Springer International Publishing, Cham, pp. 345–385. https://doi.org/10.1007/12_2015_332.
Utilisation du chanvre pour la préfabrication d'éléments de construction - ProQuest [WWW Document], n.d. URL https://www.proquest.com/docview/305036578/abstract (accessed 1.15.24).
Van Balen, K., Van Gemert, D., 1994. Modelling lime mortar carbonation. Mater. Struct. 27, 393–398. https://doi.org/10.1007/BF02473442.
Véronique, C., 2005. Propriétés mécaniques, thermiques et acoustiques d'un matériau à base de particules végétales : approche expérimentale et modélisation théorique.
Viel, M., Collet, F., Lanos, C., 2018. Chemical and multi-physical characterization of agro-resources' by-product as a possible raw building material. Ind. Crops Prod. 120, 214–237. https://doi.org/10.1016/j.indcrop.2018.04.025.
Viel, M., Collet, F., Prétot, S., Lanos, C., 2019. Hemp-straw composites: gluing study and multi-physical characterizations. Materials 12, 1199. https://doi.org/10.3390/ma12081199.
Vo, L.T.T., Navard, P., 2016. Treatments of plant biomass for cementitious building materials – a review. Construct. Build. Mater. 121, 161–176. https://doi.org/10.1016/j.conbuildmat.2016.05.125.
Wadi, H., Amziane, S., Toussaint, E., Sonebi, M., Taazount, M., 2023. Numerical analysis of timber frame wall filled with hemp concrete. Eur. J. Environ. Civ. Eng. 27, 3849–3866. https://doi.org/10.1080/19648189.2022.2162608.
Walker, R., Pavia, S., 2014. Influence of the type of binder on the properties of lime-hemp concrete. In: Llinares-Millán, C., Fernández-Plazaola, I., Hidalgo-Delgado, F., Martínez-Valenzuela, M.M., Medina-Ramón, F.J., Oliver-Faubel, I., Rodríguez-Abad, I., Salandin, A., Sánchez-Grandia, R., Tort-Ausina, I. (Eds.), Construction and Building Research. Springer, Netherlands, Dordrecht, pp. 505–514. https://doi.org/10.1007/978-94-007-7790-3_61.
Walker, R., Pavia, S., Mitchell, R., 2014. Mechanical properties and durability of hemp-lime concretes. Construct. Build. Mater. 61, 340–348. https://doi.org/10.1016/j.conbuildmat.2014.02.065.
WGBW19, 2019. World green build. Counc. https://worldgbc.org/wgbw19/.
Williams, J., Lawrence, M., Walker, P., 2018. The influence of constituents on the properties of the bio-aggregate composite hemp-lime. Construct. Build. Mater. 159, 9–17. https://doi.org/10.1016/j.conbuildmat.2017.10.109.
Williams, J., Lawrence, M., Walker, P., 2016. The influence of the casting process on the internal structure and physical properties of hemp-lime. Mater. Struct. 50, 108. https://doi.org/10.1617/s11527-016-0976-4.
Youssef, A., Picandet, V., Lecompte, T., Challamel, N., 2015. Comportement du béton de chanvre en compression simple et cisaillement. Presented at the Rencontres Universitaires de Génie Civil.
Zhang, H., Hu, J., Qi, Y., Li, C., Chen, J., Wang, X., He, J., Wang, Shuxiao, Hao, J., Zhang, Linlin, Zhang, Lijia, Zhang, Y., Li, R., Wang, Shulan, Chai, F., 2017. Emission characterization, environmental impact, and control measure of PM2.5 emitted from agricultural crop residue burning in China. J. Clean. Prod. 149, 629–635. https://doi.org/10.1016/j.jclepro.2017.02.092.
Zhang, H., Wang, Shuxiao, Hao, J., Wang, X., Wang, Shulan, Chai, F., Li, M., 2016. Air pollution and control action in Beijing. J. Clean. Prod. 112, 1519–1527. https://doi.org/10.1016/j.jclepro.2015.04.092. Preventing Smog Crises.
Zingg, L., Briffaut, M., Baroth, J., Malecot, Y., 2016. Influence of cement matrix porosity on the triaxial behaviour of concrete. Cement Concr. Res. 80, 52–59. https://doi.org/10.1016/j.cemconres.2015.10.005.
Канти, М., 2012. Binder for Manufacturing Concrete or Laminated Products.